Extremal Black Holes in Dynamical Chern-Simons Gravity

Robert McNees

Loyola University Chicago, Department of Physics, Chicago, IL 60660, USA. Kavli Institute for Theoretical Physics, University of California, Santa Barbara, CA 93106, USA.

Leo C. Stein

TAPIR, Walter Burke Institute for Theoretical Physics, California Institute of Technology, Pasadena, CA 91125, USA

Nicolás Yunes

Department of Physics, Montana State University, Bozeman, MT 59717, USA. Kavli Institute for Theoretical Physics, University of California, Santa Barbara, CA 93106, USA.

Abstract. Rapidly rotating black hole solutions in theories beyond general relativity play a key role in experimental gravity, as they allow us to compute observables in extreme spacetimes that deviate from the predictions of general relativity. Such solutions are often difficult to find in beyond-general-relativity theories due to the inclusion of additional fields that couple to the metric nonlinearly and non-minimally. In this paper, we consider rotating black hole solutions in one such theory, dynamical Chern-Simons gravity, where the Einstein-Hilbert action is modified by the introduction of a dynamical scalar field that couples to the metric through the Pontryagin density. We treat dynamical Chern-Simons gravity as an effective field theory and work in the decoupling limit, where corrections are treated as small perturbations from general relativity. We perturb about the maximally-rotating Kerr solution, the so-called extremal limit, and develop mathematical insight into the analysis techniques needed to construct solutions for generic spin. First we find closed-form, analytic expressions for the extremal scalar field, and then determine the trace of the metric perturbation, giving both in terms of Legendre decompositions. Retaining only the first three and four modes in the Legendre representation of the scalar field and the trace, respectively, suffices to ensure a fidelity of over 99% relative to full numerical solutions. The leadingorder mode in the Legendre expansion of the trace of the metric perturbation contains a logarithmic divergence at the extremal Kerr horizon, which is likely to be unimportant as it occurs inside the perturbed dynamical Chern-Simons horizon. The techniques employed here should enable the construction of analytic, closedform expressions for the scalar field and metric perturbations on a background with arbitrary rotation.

PACS numbers: 04.30.-w,04.50.Kd,04.25.-g,04.25.Nx

1. Introduction

Einstein's theory of general relativity (GR) has passed a plethora of Solar System and binary pulsar tests [1], but it has not been tested in depth in the extreme gravity regime [2, 3] where the gravitational interaction is non-linear and dynamical. A number of new observations will allow us to test this regime of Einstein's theory: in the gravitational wave spectrum through Advanced LIGO and its partners [4, 5], when compact objects collide; in the radio spectrum with the Event Horizon Telescope [6], when an accretion disk illuminates its host black hole and creates a 'shadow'; and in the X-ray spectrum with the Chandra Telescope [7], when gas heats up and glows as it accretes in the black hole spacetime. Such future observations will either confirm Einstein's theory at unprecedented levels or reveal new phenomena in the extreme gravity regime.

Solutions that represent rotating black holes (BHs) in theories of gravity beyond general relativity are an essential ingredient of tests in the extreme gravity regime. Constraining these theories requires a metric with which to calculate observables. Once a metric is available, one can investigate the modal stability of the solution, calculate the gravitational waves emitted as two BHs inspiral, compute the 'shadow' cast by a BH when illuminated by an accretion disk, and determine the energy spectrum of the radiation emitted by gas accreting into the BH.

One beyond-GR gravity theory in which generic rotating BH solutions have not yet been found is dynamical Chern-Simons (dCS) gravity [8]. This theory modifies the Einstein-Hilbert action by introducing a dynamical (pseudo) scalar field that couples non-minimally to the metric through the Pontryagin density. The interaction leads to a scalar field evolution equation that is sourced by the Pontryagin density, and modified metric field equations with third derivatives. The latter have cast doubt on whether full dCS is well-posed as an initial value problem [9], and also on whether stable BH solutions exist. We take the point of view that dCS must be treated as an effective field theory, since it is motivated from the low-energy limit of compactified heterotic string theory [10, 11] (for a review see [8]), from effective field theories of inflation [12], and from loop quantum gravity [13]. Thus the theory is treated in the decoupling limit: deformations from GR are treated perturbatively, reducing the order of the field equations.

When treated as an effective theory, BH solutions in dCS have been found in certain limits. A non-rotating BH was found by Jackiw and Pi [14], who showed that the Schwarzschild metric is also a solution of dCS. Linear stability of high-frequency waves about the Schwarzschild background was suggested by [15]. The first investigations of rotating solutions assumed a small rotation parameter. The axionic hair on a slowly-rotating BH was found in [16]. Later, the metric solution to linear order in spin was found independently by Yunes and Pretorius [17], and Konno, et al. [18]. This solution was extended to quadratic order by Yagi, Yunes and Tanaka [19]. More recently, Konno and Takahashi [20] and Stein [21] investigated the behavior of the dynamical scalar field about a rapidly rotating Kerr background. Stein also investigated the trace of the metric perturbation, and found that the extremal limit may be singular, which partly motivated the present work.

At present, nobody has succeeded in constructing the full metric of generic rotating BHs in dCS gravity, despite over two decades of work in that direction [16, 14, 22, 23, 24, 17, 18, 19, 20, 21]. The general procedure for obtaining the metric in the decoupling limit is simple enough. First, one finds the leading order behavior of the scalar field

as sourced by the background geometry. The scalar field determines the source for the leading order term in the deformation of the metric, which must then be solved for. But progress has been limited because the initial step has proven difficult; the scalar field satisfies a complicated partial differential equation on the Kerr background, and only partial results have been obtained for finite rotation. Therefore, if the goal is to find a complete description for the metric deformation, then a full solution for the scalar field is an unavoidable first step.‡

For all of these reasons, as a first step toward finding full rotating BH solutions in effective dCS gravity, we study the scalar field on a background where the BH spin takes the maximal Kerr value. This extremal limit is of interest not only because the mathematics simplify significantly, but also because of the Kerr/CFT conjecture that posits a dual holographic description in terms of a two-dimensional conformal field theory [25, 26, 27, 28, 29, 30]. Working in the extremal limit, we obtain a general, closed-form expression for the Legendre modes of the scalar field. The radial structure of the scalar field is more complicated than that of the slowly-rotating case. Whereas the slowly-rotating case only requires a finite polynomial expansion, the rapid-rotation case is characterized by natural logarithms and arctangents. And unlike the slowlyrotating case, where the scalar field is primarily dipolar, the octupole mode of the field on the extremal background carries more than half of the field's ADM energy. We find that retaining the first 3 non-vanishing Legendre modes of the scalar field is necessary to achieve a fidelity above 99% in the entire domain relative to the full numerical solution. Our results for the scalar field complete the first step in the process outlined above and establish a viable starting point for either an analytic or numerical treatment of the dCS metric deformation of the extremal Kerr solution.

With analytic, closed-form expressions for the extremal scalar field in hand, we turn our attention to the BH metric. Treating the dCS correction as a small perturbation of the Kerr background and working in a convenient (Lorenz-like) gauge, we show that the modified field equations for the trace of the metric perturbation can be solved in quadrature in terms of another Legendre mode decomposition. As in the scalar field case, the radial structure of the metric perturbation is quite different from that of slowly-rotating BHs. In particular, the dominant monopole mode exhibits a logarithmic divergence at the extremal Kerr horizon, which confirms a conjecture made in [21] by one of the authors. This divergence, however, may be unphysical because the Kerr horizon is likely "inside" the perturbed dCS horizon. Away from this region, the angular structure of the trace of the metric perturbation is predominantly monopolar, with higher order modes modes playing a more important role than in the slowly-rotating case. We find that retaining the first 4 non-vanishing modes of the trace of the metric perturbation achieves a fidelity above 99% in the entire domain relative to the full numerical solution.

Although the trace of the metric perturbation is not a gauge-invariant observable quantity, and although we have not yet analyzed the full metric perturbation, the calculation of the trace establishes two useful results. First, the techniques used to solve the equation of motion for the scalar field are also applicable to the scalar degree of

[‡] A more modest approach might be to construct a reliable analytical approximation for the metric. But this requires understanding the scalar field well enough to ensure that the source terms for the metric, which depend on the scalar, are rendered with sufficient detail. And even if the goal is to develop a purely numerical description of the metric, some basic understanding of the scalar is still needed to test the robustness of the simulations. Before we can attack the problem of the metric deformation, then, we must first make more progress on solving the general problem of the scalar field.

freedom in the metric perturbation. This suggests that similar techniques can probably also be used to solve for the other degrees of freedom of the metric perturbation, and work along these lines is currently underway. Second, it appears that only a small number of modes are necessary to accurately approximate both the scalar field and the metric perturbation. This suggests that an excellent approximation to a full numerical solution for the metric perturbation could be achieved through a spectral decomposition that retains a finite number of modes.

The results we have obtained also have various other consequences for the study of BHs in dCS gravity and other beyond-GR gravity theories. First, the techniques used to solve for the scalar field on the extremal Kerr background can be applied to subsequent terms in a near-extremal expansion in dCS gravity. More importantly, these techniques generalize to backgrounds with arbitrary rotation parameter [21], as well as other higher-curvature interactions. Some of our results have already been extended to backgrounds with arbitrary spin, and will be presented elsewhere [31] Second, the scalar degree of freedom in the metric perturbation can be studied using the same methods we employed for the scalar field. It seems likely that the vector and transverse-traceless components of the metric perturbation can be analyzed using similar techniques, and that these techniques can also be applied to Einstein-dilaton-Gauss-Bonnet gravity and other quadratic gravity theories [32, 33, 34, 35, 36, 37, 38]. Third, the logarithmic divergence of the trace of the metric suggests a conjecture: that the dCS-corrected horizon is "outside" of the Kerr horizon for all possible values of angular momentum, protecting against a naked singularity. The verification of this conjecture will require further work that utilizes the solution for the full metric perturbation. And finally, our results also suggest that generic rotating BH solutions in beyond-GR theories will not have the simple rational-polynomial form that the Kerr metric enjoys, and may require more complicated functional forms. If true, this would imply that the simple parameterized metrics used to constrain GR deviations with Event Horizon Telescope observations of the BH shadows cannot be used to constrain quadratic gravity theories.

The remainder of this paper presents details of the techniques developed, the solutions obtained, and their properties. Henceforth, we use the following conventions. Latin letters (a, b, c, ...) in index lists stand for spacetime indices. Parentheses and square brackets in index lists stand for symmetrization and anti-symmetrization respectively. The metric signature will be (-, +, +, +) and we choose units in which c = 1. However, we do not set G or h to unity. All other conventions follow the standard treatment of [39, 40].

2. The ABC of dCS

Dynamical Chern-Simons gravity [14, 8] is a four-dimensional theory defined by the action

$$I = I_{\text{EH}} + I_{\text{CS}} + I_{\vartheta} + I_{\text{Mat}}. \tag{1}$$

The first term is the Einstein-Hilbert action

$$I_{\rm EH} = \int d^4x \, \sqrt{-g} \, \left(\frac{1}{2\kappa^2} R\right) \,, \tag{2}$$

where $\kappa^2 = 8\pi G$, R is the Ricci scalar associated with the metric tensor $g_{\mu\nu}$, and g is the metric determinant. The last term in Eq. (1) is the action for all matter degrees of freedom, which couple minimally to the metric tensor and do not couple to ϑ .

The Chern-Simons correction is mediated by a canonically-normalized scalar field ϑ , whose kinetic term in the action is

$$I_{\vartheta} = \int d^4x \sqrt{-g} \left(-\frac{1}{2} \left(\partial_a \vartheta \right) \left(\partial^a \vartheta \right) \right) . \tag{3}$$

This scalar field couples non-minimally to the metric through the term in the action

$$I_{\rm CS} = \int d^4x \sqrt{-g} \, \left(-\frac{1}{4} \frac{\alpha}{\kappa} \, \vartheta \, *RR \right) \,, \tag{4}$$

where the Pontryagin density is defined via

$$*RR := *R^{abcd}R_{abcd} = \frac{1}{2}\epsilon^{abef}R_{ef}^{\ cd}R_{abcd}, \qquad (5)$$

and ϵ^{abcd} is the Levi-Civita tensor. Notice that the definition of the Pontryagin density here differs from that of [8] by a minus sign, which is compensated by an additional minus sign in I_{CS} .

Variation of the action with respect to the metric yields the field equations

$$G_{ab} + 2 \alpha \kappa C_{ab} = \kappa^2 T_{ab} \,, \tag{6}$$

where G_{ab} is the Einstein tensor, and the traceless 'C-tensor' is defined as

$$C^{ab} = (\nabla_c \vartheta) \epsilon^{cde(a} \nabla_e R^{b)}_d + (\nabla_c \nabla_d \vartheta) *R^{d(ab)c}.$$
 (7)

The stress-energy tensor decomposes linearly into a term that depends only on the matter degrees of freedom and a term that depends only on the scalar field, i.e. $T_{ab} = T_{ab}^{\text{Mat}} + T_{ab}^{\vartheta}$, where the latter is

$$T_{ab}^{\vartheta} := (\nabla_a \vartheta) (\nabla_b \vartheta) - \frac{1}{2} g_{ab} (\nabla_c \vartheta) (\nabla^c \vartheta) . \tag{8}$$

Variation of the action with respect to the scalar field yields its evolution equation

$$\square \vartheta = \frac{\alpha}{4\kappa} *RR, \qquad (9)$$

where \square stands for the d'Alembertian operator. Notice that there is no potential associated with the scalar field, which implies it is a long-ranged field. This vanishing (or flat) potential means that ϑ retains a global shift symmetry, $\vartheta \to \vartheta + \text{const.}$, because *RR is related to a topological invariant [41]. Retaining this shift symmetry may be important to protect against certain quantum corrections.

The theoretical motivation to study dCS is varied. From a string-theory standpoint, non-minimal scalar couplings of the form of Eq. (4) arise in the low-energy limit of heterotic string theory upon four-dimensional compactification [10, 11] (for a review see [8]). From a loop quantum gravity standpoint, dCS arises when the Barbero-Immirzi parameter is promoted to a scalar field in the presence of fermions [13, 42]. From a cosmology standpoint, the interaction in Eq. (4) arises as one of three terms that remain in an effective field theory treatment of single-field inflation [12].

The choice of conventions made here differs from that of [8]. The mapping between the two sets is $\kappa_{AY} = 1/(2\kappa^2)$, $\beta_{AY} = 1$ and $\alpha_{AY} = \alpha/\kappa$. Moreover, we retain all factors of G, or equivalently of κ , since we do not set G to unity. Without requiring the action to have any specific sets of units, demanding consistency between I_{EH} , I_{CS} and I_{ϑ} implies $[\vartheta] = [\kappa]^{-1}$ and $[\alpha] = L^2$, where L stands for units of length. Given some GR solution with characteristic length scale \mathcal{L} , corrections are then controlled by the dimensionless parameter $\zeta := \alpha^2/\mathcal{L}^4$. One can see this by noting that $|\partial_{ab}\vartheta| \propto (\alpha/\kappa)\mathcal{L}^{-4}$ from Eq. (9), which implies that $|C_{ab}| \propto (\alpha/\kappa)\mathcal{L}^{-6}$ from Eq. (7). Then the fractional corrections to GR are proportional to $(\alpha\kappa|C_{ab}|/|G_{ab}|) \propto \alpha^2\mathcal{L}^{-4} = \zeta$.

Current constraints on dCS are rather weak because dCS corrections are relevant only in scenarios where the spacetime curvature is large. One can see this by noting that dCS corrections to the gravitational field are sourced by the scalar field, which in turn is only sourced by the spacetime curvature. In fact, one can easily show through the argument given in the previous paragraph that constraints on the α parameter of dCS will be roughly proportional to a power of \mathcal{L} . Let us assume that some observation places the constraints $|\zeta| < \delta$, where δ is related to the observation and its uncertainties. This constraint can then be mapped to a constraint on α to find $\sqrt{|\alpha|} < \delta^{1/4}\mathcal{L}$. Currently, the best constraint on the dCS coupling parameter is $\sqrt{|\alpha|} \lesssim 10^8$ km and it comes from observations of Lense-Thirring precession from satellites in orbit around Earth [43]. Such a weak constraint makes sense when one realizes that for these kind of experiments the characteristic length scale $\mathcal{L} = [R_{\oplus}^3/(GM_{\oplus})]^{1/2} \approx 2 \times 10^8$ km. Binary pulsar observations cannot yet be used to constrain the theory because modifications to the orbital dynamics are too weak and couple to the spin of the bodies [44].

The aforementioned theoretical motivations suggest that one treat dCS as an effective theory valid up to some cut-off scale, i.e., the scale above which higher-order curvature terms in the action cannot be neglected [2, 3]. We will here restrict attention to physical scenarios in which the effective theory is valid, and since we are interested only in black holes, this means we restrict attention to those with masses $GM \gg \sqrt{\alpha}$. When this is the case, we can work in the decoupling limit of the theory, i.e. we perform a perturbative expansion of the field equations and their solutions in powers of ζ . Henceforth, dCS is exclusively treated in the decoupling limit.

The decoupling limit can be implemented in practice by expanding the metric tensor and the scalar field in powers of ζ . In this paper, we will expand the metric and the scalar field as follows:

$$g_{ab} = g_{ab}^{(0)} + \zeta^{1/2} g_{ab}^{(1/2)} + \zeta g_{ab}^{(1)} + \mathcal{O}(\zeta^{3/2}), \qquad (10)$$

$$g_{ab} = g_{ab}^{(0)} + \zeta^{1/2} g_{ab}^{(1/2)} + \zeta g_{ab}^{(1)} + \mathcal{O}(\zeta^{3/2}), \qquad (10)$$

$$\vartheta = \frac{1}{\kappa} \tilde{\vartheta}^{(0)} + \frac{1}{\kappa} \zeta^{1/2} \tilde{\vartheta}^{(1/2)} + \frac{1}{\kappa} \zeta \tilde{\vartheta}^{(1)} + \mathcal{O}(\zeta^{3/2}), \qquad (11)$$

where the superscript denotes the order in ζ of each term. Notice that a factor of κ^{-1} in the expansion for the scalar field ensures that $\tilde{\vartheta}^{(n)}$ is dimensionless. As we are perturbing about $\zeta = 0$, our background solution $(g^{(0)}, \tilde{\vartheta}^{(0)})$ must solve the field equations for GR and a free massless scalar field. Choosing trivial initial data for $\tilde{\vartheta}^{(0)}$ gives $\tilde{\vartheta}^{(0)}=0$ at all times, so we find $(g_{ab}^{(0)},\tilde{\vartheta}^{(0)})=(g_{ab}^{\rm GR},0)$ at zeroth order, where $g_{ab}^{\rm GR}$ is some known GR solution. If we next examine the system at order $\zeta^{1/2}$, we find that $g_{ab}^{(1/2)}$ satisfies a homogeneous linear equation due to the vanishing of $\tilde{\vartheta}^{(0)}$. Therefore, again, trivial initial data gives $g_{ab}^{(1/2)} = 0$ at all times.

Thus to the order we are working, our expansion is

$$g_{ab} = g_{ab}^{GR} + \zeta g_{ab}^{(1)} + \mathcal{O}(\zeta^{3/2}),$$
 (12)

$$\vartheta = 0 + \frac{1}{\kappa} \zeta^{1/2} \, \tilde{\vartheta}^{(1/2)} + \mathcal{O}(\zeta^1) \,.$$
(13)

Henceforth, we will focus on BH solutions, with the $\mathcal{O}(\zeta^0)$ term in the metric, g_{ab}^{GR} , being simply the Kerr metric. The $\mathcal{O}(\zeta^{1/2})$ term in the scalar field, $\vartheta^{(1/2)}$, is sourced by the Kerr metric and, in turn, this sources the $\mathcal{O}(\zeta)$ correction to the metric, $g_{ab}^{(1)}$. To be within the regime of validity of the perturbative expansion, we require $\zeta \ll 1$, and since for the Kerr black hole the typical curvature length scale is $\mathcal{L} = GM$, we take

$$\zeta = \frac{\alpha^2}{(GM)^4} \ll 1. \tag{14}$$

Notice that this definition differs from others in the literature [8] in that we do not include a factor of $1/\kappa^2$ in ζ , but rather we factor it out in the scalar field directly.

In this paper we are concerned with solutions that represent rotating BHs spinning near extremality, so in addition to the decoupling expansion we will also perform a near-extremal expansion. Letting the (z-component of the) BH spin angular momentum be J_z , we can define the BH dimensionless spin parameter $\chi := J_z/(GM)^2$. We can then expand all fields in the problem in a bivariate expansion, i.e. a simultaneous expansion in both $\zeta \ll 1$ and $\chi \sim 1$, namely

$$g_{ab}^{(n)} = g_{ab}^{(n,0)} + \varepsilon g_{ab}^{(n,1)} + \varepsilon^2 g_{ab}^{(n,2)} + \mathcal{O}(\varepsilon^3),$$

$$\tilde{\vartheta}^{(n)} = \tilde{\vartheta}^{(n,0)} + \varepsilon \tilde{\vartheta}^{(n,1)} + \varepsilon^2 \tilde{\vartheta}^{(n,2)} + \mathcal{O}(\varepsilon^3),$$
(15)

$$\tilde{\vartheta}^{(n)} = \tilde{\vartheta}^{(n,0)} + \varepsilon \, \tilde{\vartheta}^{(n,1)} + \varepsilon^2 \, \tilde{\vartheta}^{(n,2)} + \mathcal{O}(\varepsilon^3) \,, \tag{16}$$

where $\varepsilon := (1-\chi^2)^{1/2}$ is a near-extremality parameter and $\varepsilon \ll 1$ for near-extremal

3. Scalar Field: Solution

We wish to solve the evolution equation for the scalar field [Eq. (9)] to leading order in ζ . To this order, the Pontryagin density on the right-hand side of Eq. (9) is evaluated on the unmodified Kerr spacetime. The wave operator on the left-hand side can also be evaluated on the Kerr spacetime, since corrections will be of $\mathcal{O}(\zeta)$. In polynomial Boyer-Lindquist coordinates, the scalar field evolution equation is evaluated on the line element [45]

$$g_{ab}^{(0)} dx^a dx^b = -\frac{\Delta}{\Sigma} \left[dt - a \Gamma d\phi \right]^2 + \frac{\Sigma}{\Delta} dr^2 + \frac{\Sigma}{\Gamma} d\psi^2 + \frac{\Gamma}{\Sigma} \left((r^2 + a^2) d\phi - a dt \right)^2, \quad (17)$$

where the usual polar angle θ has been replaced with a coordinate $\psi = \cos \theta$, and $\Gamma := 1 - \psi^2 = \sin^2 \theta$. The mass of the black hole is M and it rotates with angular momentum per unit mass $a = J_z/(GM)$, where $-GM \le a \le GM$. The functions Σ and Δ are

$$\Sigma = r^2 + a^2 \psi^2 \tag{18}$$

$$\Delta = r^2 - 2GMr + a^2 \,, \tag{19}$$

so that the background horizons, where $\Delta = (r - r_+)(r - r_-) = 0$, are located at $r_{\pm} = GM \pm \sqrt{(GM)^2 - a^2}$.

It will be convenient to replace all quantities with dimensionless variables by scaling out factors of GM: $\tilde{r} = r/(GM)$ and $\chi = a/(GM)$, so that the rescaled functions $\tilde{\Delta} = \Delta/(GM)^2 = (\tilde{r}-1)^2 - (1-\chi^2)$ and $\tilde{\Sigma} = \Sigma/(GM)^2 = \tilde{r}^2 + \chi^2 \psi^2$. Assuming a stationary and axisymmetric solution for the scalar field, the $\mathcal{O}(\alpha)$ term in Eq. (9) then takes the form

$$\partial_{\tilde{r}}(\tilde{\Delta}\partial_{\tilde{r}}\tilde{\vartheta}^{(1/2)}) + \partial_{\psi}(\Gamma\partial_{\psi}\tilde{\vartheta}^{(1/2)}) = s^{(1/2)}(\tilde{r},\psi) \tag{20}$$

where factors of (α/κ) and (GM) have canceled from both sides of the equation. The source $s^{(1/2)}(\tilde{r},\psi)$ is proportional to Σ (* $RR^{(0)}$) and given explicitly by

$$s^{(1/2)}(\tilde{r},\psi) = 24 \frac{\chi \tilde{r} \psi (3\tilde{r}^2 - \chi^2 \psi^2)(\tilde{r}^2 - 3\chi^2 \psi^2)}{\tilde{\Sigma}^5} . \tag{21}$$

Equation (20) admits a solution via separation of variables, by expanding the solution

$$\tilde{\vartheta}^{(1/2)} = \sum_{\ell=0}^{\infty} \tilde{\vartheta}_{\ell}^{(1/2)}(\tilde{r}) P_{\ell}(\psi) , \qquad (22)$$

where $P_{\ell}(\cdot)$ are Legendre functions of the first kind. The radial modes $\tilde{\vartheta}_{\ell}^{(1/2)}(\tilde{r})$ then satisfy the equation

$$\partial_{\tilde{r}} \left(\tilde{\Delta} \partial_{\tilde{r}} \tilde{\vartheta}_{\ell}^{(1/2)} \right) - \ell(\ell+1) \tilde{\vartheta}_{\ell}^{(1/2)} = s_{\ell}^{(1/2)}(\tilde{r}) , \qquad (23)$$

with source functions $s_\ell^{(1/2)}(\tilde r)$ given by the modes in the Legendre decomposition of Eq. (21)

$$s_{\ell}^{(1/2)}(\tilde{r}) = \frac{2\ell+1}{2} \int_{-1}^{1} d\psi \, P_{\ell}(\psi) s^{(1/2)}(\tilde{r}, \psi) . \tag{24}$$

Note that the source function in Eq. (21) is odd in the variable ψ , so its Legendre expansion (as well as that of the scalar field) will only contain odd modes: $\ell = 2n + 1$ for all $n \in \mathbb{N}$.

The integral in Eq. (24) can be evaluated in closed form in terms of known functions:

$$s_{\ell}^{(1/2)}(\tilde{r}) = (-1)^{\frac{\ell+1}{2}} \frac{\Gamma(\frac{1}{2})\Gamma(\ell+4)}{2^{\ell}\Gamma(\ell+\frac{1}{2})} \frac{\chi^{\ell}}{\tilde{r}^{\ell+4}} \left[3 {}_{2}F_{1}\left(\frac{\ell+4}{2}, \frac{\ell+5}{2}; \ell+\frac{3}{2}; -\frac{\chi^{2}}{\tilde{r}^{2}}\right) - (\ell+5) {}_{2}F_{1}\left(\frac{\ell+4}{2}, \frac{\ell+7}{2}; \ell+\frac{3}{2}; -\frac{\chi^{2}}{\tilde{r}^{2}}\right) \right], \quad (25)$$

where ${}_2F_1(\cdot,\cdot;\cdot;\cdot)$ is the ordinary hypergeometric function and ℓ is odd. One can show, via identities for hypergeometric functions, that this expression is equivalent to one given previously in [46]. Note that the hypergeometric functions go to unity in the $\tilde{r} \to \infty$ limit, so that the leading behavior at large \tilde{r} is given by $s_{\ell}^{(1/2)}(\tilde{r}) \sim \tilde{r}^{-(\ell+4)}$.

The solution of Eq. (23) can be obtained through the method of variation of parameters (see Appendix A). Defining a new variable $\eta = (\tilde{r} - 1)/\sqrt{1 - \chi^2}$, the

solution of Eq. (23) [see also Eq. (A.3)] for the mode function $\tilde{\vartheta}_{\ell}^{(1/2)}$ is

$$\tilde{\vartheta}_{\ell}^{(1/2)}(\tilde{r}) = P_{\ell}(\eta) \int_{\infty}^{\eta} d\eta' \, s_{\ell}^{(1/2)}(1 + \eta' \sqrt{1 - \chi^2}) \, Q_{\ell}(\eta') \\
- Q_{\ell}(\eta) \int_{1}^{\eta} d\eta' \, s_{\ell}^{(1/2)}(1 + \eta' \sqrt{1 - \chi^2}) \, P_{\ell}(\eta') \,, \quad (26)$$

where $Q_{\ell}(\cdot)$ are Legendre functions of the second kind. This solution is regular at \tilde{r}_{+} , and approaches zero as $\tilde{r} \to \infty$.

Our eventual goal is to evaluate Eq. (26) in closed form for the full range of the rotation parameter, $-1 \le \chi \le 1$. The slow rotation limit of the field, i.e. the solution in a $|\chi| \ll 1$ expansion, is already well-understood; it was first derived in [17], verified in [18], and extended to second order in rotation in [19]. Similarly, it is also possible to systematically solve the scalar field equation of motion in the near-extremal expansion introduced in Sec. 2. Expanding the source functions of Eq. (25) for $\varepsilon \ll 1$, we find

$$s_{\ell}^{(1/2)}(\tilde{r}) = s_{\ell}^{(1/2,0)}(\tilde{r}) + \varepsilon^2 s_{\ell}^{(1/2,2)}(\tilde{r}) + \varepsilon^4 s_{\ell}^{(1/2,4)}(\tilde{r}) + \mathcal{O}(\varepsilon^6). \tag{27}$$

Recall that the second superscript in each of these terms represents the order in ε at which it enters the near-extremal expansion. Because the $\chi \to 1$ limit is regular for $s_{\ell}^{(1/2)}(\tilde{r}), s_{\ell}^{(1/2,0)}(\tilde{r})$ is simply $s_{\ell}^{(1/2)}(\tilde{r})$ evaluated at $\chi = 1$.

In this paper we will only consider the extremal limit, $\varepsilon \to 0$, which is the leading term in the near-extremal expansion. This corresponds to the limit $\chi \to \pm 1$ of the dimensionless spin parameter χ . The homogeneous solutions are regular in this limit [see Eqs. (A.8)-(A.9)], and the solution for the scalar field [see Eq. (A.3)] at $\varepsilon = 0$ is

$$\tilde{\vartheta}_{\ell}^{(1/2,0)}(\tilde{r}) = \frac{1}{2\ell+1} \left[(\tilde{r}-1)^{\ell} \int_{\infty}^{\tilde{r}} d\tilde{r}' \frac{s_{\ell}^{(1/2,0)}(\tilde{r}')}{(\tilde{r}'-1)^{\ell+1}} - \frac{1}{(\tilde{r}-1)^{\ell+1}} \int_{1}^{\tilde{r}} d\tilde{r}' (\tilde{r}'-1)^{\ell} s_{\ell}^{(1/2,0)}(\tilde{r}') \right] . \quad (28)$$

The source functions at leading-order in ε , $s_{\ell}^{(1/2,0)}(\tilde{r})$, are given by Eq. (24) or Eq. (25) evaluated at $|\chi|=1$. The boundary conditions are the same as before: each mode $\tilde{v}_{\ell}^{(1/2,0)}$ is regular at $\tilde{r}_{+}=1$, and goes to zero as $\tilde{r}\to\infty$.

The integrals in Eq. (28) can be readily evaluated for specific values of ℓ . For example, the $\ell=1$ radial mode is given by

$$\tilde{\vartheta}_{1}^{(1/2,0)}(\tilde{r}) = 3(\tilde{r}-1)\log\left(\frac{\tilde{r}-1}{\sqrt{\tilde{r}^{2}+1}}\right) + 3(\tilde{r}-1)\operatorname{arccot}\tilde{r} + \frac{3(\tilde{r}-1)(2\tilde{r}^{2}+\tilde{r}+3)}{2(\tilde{r}^{2}+1)^{2}}.$$
(29)

With more work, we can also give an expression for general values of ℓ in terms of finite-order rational polynomials, $\operatorname{arccot}(\tilde{r})$, and the log which appears above. But before we can give the general form, we first have to establish a few results for the behavior of the modes at large \tilde{r} and at $\tilde{r} = 1$.

The far-field behavior of the modes is dominated by the second line of Eq. (28), since the term in the first line decays with a higher power of r. The integral in the

second line converges in this limit, and thus, $\tilde{\vartheta}_{\ell}^{(1/2,0)} \sim \tilde{r}^{-(\ell+1)}$ as $\tilde{r} \gg 1$. Notice, though, that this asymptotic behavior is not immediately apparent in our initial result, Eq. (29). In that case the individual terms fall off more slowly than \tilde{r}^{-2} , but cancellations between the terms result in the correct asymptotic behavior. The same will be true for our result for general ℓ : individual terms may not behave as $\tilde{r}^{-(\ell+1)}$ at large \tilde{r} , but cancellations between these terms will give the correct result.

The near-horizon behavior of the modes is dominated by the first integral in Eq. (28), but its asymptotic behavior as $\tilde{r} \sim 1$ cannot be easily discerned from that equation. Instead, it is easier to return to Eq. (26) and set $\chi = 1$, remembering that the horizon limit $\tilde{r} \to 1$ is equivalent to $\eta \to 1$ (this is the case for all values of χ). In this limit, only the first line of Eq. (26) contributes, leading to

$$\tilde{\vartheta}_{\ell}^{(1/2,0)}(1) = -\frac{1}{\ell(\ell+1)} s_{\ell}^{(1/2,0)}(1) . \tag{30}$$

The overall ℓ -dependent factor comes from the definite integration of $Q_{\ell}(\eta')$ in the range $\eta' \in (1, \infty)$, while $s_{\ell}^{(1/2, 0)}(1)$ is Eq. (25) evaluated at $\chi = 1$ and $\tilde{r} = 1$. As a check of this result, it is instructive to consider the behavior of the scalar field in the Near-Horizon Extremal Kerr (NHEK) limit [47, 25]. At extremality, regularity of the field at the horizon insures that the first term on the left-hand-side of Eq. (20) vanishes as $\tilde{r} \to 1$. Then the ψ -dependence of the scalar field in this limit is determined by

$$\partial_{\psi} \left(\Gamma \partial_{\psi} \tilde{\vartheta}^{(1/2, 0)}(1, \psi) \right) = s^{(1/2, 0)}(1, \psi) = \frac{24 \,\tilde{r} \,\psi \,(3 - \psi^2)(1 - 3\psi^2)}{(1 + \psi^2)^5} \ . \tag{31}$$

The inhomogeneous solution can be obtained by direct integration, and the full solution that is regular on $-1 \le \psi \le 1$ is given by

$$\tilde{\vartheta}^{(1/2,0)}(1,\psi) = -\frac{4\psi}{(1+\psi^2)^3} + \frac{\psi}{2(1+\psi^2)} + \arctan(\psi) \ . \tag{32}$$

It is straightforward to check that this agrees with the Legendre series Eq. (22), with coefficients given by Eq. (30) for the mode functions at the horizon.

With these results, we can now give a general expression for the radial modes of the scalar field. They take the form

$$\tilde{\vartheta}_{\ell}^{(1/2,0)}(\tilde{r}) = A_{\ell}(\tilde{r}) + B_{\ell}(\tilde{r}) \operatorname{arccot}(\tilde{r}) + C_{\ell}(\tilde{r}) \log \left(\frac{\tilde{r} - 1}{\sqrt{\tilde{r}^2 + 1}}\right) , \tag{33}$$

where the functions $A_{\ell}(\tilde{r})$, $B_{\ell}(\tilde{r})$, and $C_{\ell}(\tilde{r})$ are

$$A_{\ell}(\tilde{r}) = (-1)^{\frac{\ell-1}{2}} \frac{\ell(\ell-1)}{(\tilde{r}-1)^{\ell+1}} \sum_{k=0}^{\ell} \gamma_k (\tilde{r}-1)^k + \sum_{k=0}^{\ell-1} \alpha_{\ell,k} \, \tilde{r}^k$$

$$-\frac{2\ell+1}{(\tilde{r}^2+1)^2} + \frac{(2\ell+1)(4\tilde{r}-\ell(\ell+1))}{4(\tilde{r}^2+1)}$$
(34)

$$B_{\ell}(\tilde{r}) = (-1)^{\frac{\ell+1}{2}} \frac{\ell(\ell-1)}{(\tilde{r}-1)^{\ell+1}} + \sum_{k=0}^{\ell} \beta_{\ell,k} \, \tilde{r}^k$$
 (35)

$$C_{\ell}(\tilde{r}) = (-1)^{\frac{\ell-1}{2}} \frac{(\ell+1)(\ell+2)}{2} (\tilde{r}-1)^{\ell}.$$
 (36)

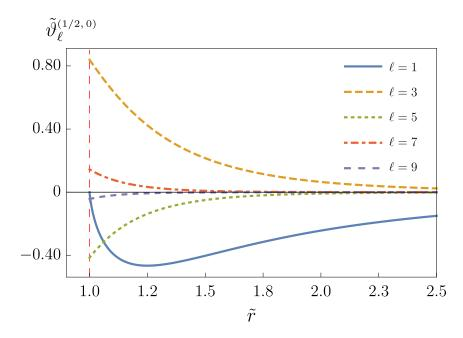


Figure 1. The first five radial mode functions of the scalar field. The vertical dashed line indicates the location of the event horizon of an extremal black hole. The $\ell=1$ mode vanishes at the horizon, while modes with $\ell>1$ are all non-zero at $\tilde{r}=1$.

The constants γ_k appearing in $A_\ell(\tilde{r})$ are the first $\ell+1$ terms in the Taylor expansion of $\operatorname{arccot}(\tilde{r})$ around $\tilde{r}=1$

$$\gamma_k = \frac{1}{k!} \left(\frac{\partial}{\partial x^k} \operatorname{arccot}(x) \right) \bigg|_{x=1} .$$
(37)

The remaining $2\ell+1$ coefficients $\alpha_{\ell,k}$ and $\beta_{\ell,k}$ are fixed by imposing the boundary conditions: each mode falls off as $\tilde{r}^{-(\ell+1)}$ at large \tilde{r} , and takes the value Eq. (30) at $\tilde{r}=1$. Alternately, the condition at $\tilde{r}=1$ can be replaced with the requirement that the leading asymptotic behavior of the mode is given by Eq. (C.25). The coefficients $\alpha_{\ell,k}$ and $\beta_{\ell,k}$ for the first several modes are given explicitly in Appendix B.

4. Scalar Field: Properties

Let us now discuss some properties of the scalar field solution obtained in the previous section. We begin by plotting the first five (odd) modes in Fig. 1. Observe that the integrated norm of $\tilde{\vartheta}_{\ell}^{(1/2,\,0)}$ decays exponentially with ℓ . This is because this function is a spectral solution to a differential equation with a C^{∞} source, so it must converge exponentially with mode number. Observe also from Fig. 1 that the $\ell=1$ mode of the field vanishes at the horizon. Modes with $\ell>1$ are finite but non-zero at the horizon, with values that scale like $\ell^{5/2}(1+\sqrt{2})^{-(\ell+1)}$ for $\ell\gg 1$.

By including contributions from a sufficient number of modes, we can construct an arbitrarily accurate approximation of the full, extremal scalar field. An approximation

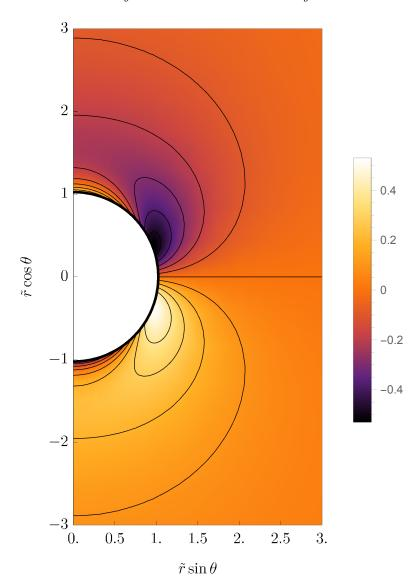


Figure 2. The behavior of the scalar field on the extremal background, approximated by its first five Legendre modes. The coordinates $\tilde{r}\psi$ and $\tilde{r}\sqrt{1-\psi^2}$ correspond to $\tilde{r}\cos\theta$ and $\tilde{r}\sin\theta$, respectively, in conventional Boyer-Lindquist coordinates.

using the first five modes is shown in Fig. 2, as a function of both radius and polar angle. Notice the similarity to Fig. 3 of Stein [21], resulting from a numerical solution at large but not extremal ($\chi = 0.999$) rotation; we will discuss this more below. The accuracy of this approximation can be characterized using a slicing-independent measure of the scalar field energy through the ADM energy. Let u^a be a timelike unit vector normal to a hypersurface \mathcal{S} , with γ_{ab} the induced metric on \mathcal{S} . Then the scalar field's

contribution to the energy is

$$E = \int_{S} d^3x \,\sqrt{\gamma} \,u^a T^{\vartheta}_{ab} t^b \tag{38}$$

where t^b is the Killing vector $\partial/\partial t$. This energy can be perturbatively expanded in powers of ζ ,

$$E = \zeta E^{(1)} + \zeta^2 E^{(2)} + \dots \tag{39}$$

The scalar field's ADM energy at leading order can further be computed via the spectral decomposition,

$$E^{(1)} = M \sum_{k=1}^{\infty} \tilde{E}_k^{(1)}, \tag{40}$$

with the dimensionless $\tilde{E}_k^{(1)}$ functions given by

$$\tilde{E}_{k}^{(1)} = \frac{1}{4} \frac{1}{2k+1} \int_{\tilde{r}_{\perp}}^{\infty} d\tilde{r} \left[\tilde{\Delta} (\partial_{\tilde{r}} \tilde{\vartheta}_{k}^{(1/2)})^{2} + k(k+1) (\tilde{\vartheta}_{k}^{(1/2)})^{2} \right]. \tag{41}$$

The fractional difference between the total energy in the scalar field and the energy in the first N modes is then

$$\delta_N = 1 - \frac{M}{E^{(1)}} \sum_{k=1}^N \tilde{E}_k^{(1)} . \tag{42}$$

Figure 3 shows the fractional difference δ_N for the first seven nonvanishing modes. The contribution from the first five – up to $\ell=9$ – differs from the total energy by less than one part in 10^4 . Observe that the accuracy increases exponentially with N. Observe also that if we wish to capture 99% of the energy in the field, it suffices to keep only up to the first three odd modes, i.e. N=5. Finally, note that the energy in the scalar field is dominated by the behavior of the scalar field close to the horizon. If one is interested in regimes of spacetime outside some two-sphere with radius $r\gg M$, then the full scalar field can be accurately modeled using just the dipole ($\ell=1$) and octupole ($\ell=3$) modes.

Let us briefly compare these analytic results at extremality with numerical results away from extremality, which were computed in Stein [21]. First, we have performed a direct comparison of the analytical calcuation presented here with the numerics in [21]. Because of the numerical method of [21], those results must be at values of $|\chi| < 1$. Specifically, we compared the analytical results presented here with numerical results computed with the highest spin of $\chi = 1 - 10^{-10}$ (extremality parameter approximately $\varepsilon \approx \sqrt{2} \times 10^{-5}$), with $N_{ang} = 64$ angular and $N_x = 1024$ radial collocation points (high spins require very high radial resolution). Comparisons against lower resolutions show that these results are converging. This comparison is displayed in Fig. 4. We see that even at the extremality parameter $\varepsilon \approx \sqrt{2} \times 10^{-5}$, the numerical solution is converging to the regular analytic solution. The nonzero fractional differences in Fig. 4 should decrease in the limit as $\varepsilon \to 0$ and in the continuum limit $N_x \to \infty$.

We can also use the numerical method of [21] to show convergence to the extremal limit, which is regular. This is demonstrated in Fig. 5 as a function of the rotation of

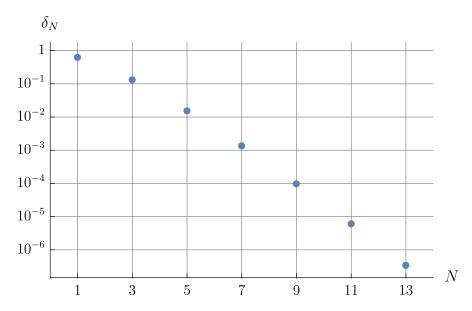


Figure 3. The fractional difference between the scalar field's contribution to the ADM energy, and the contribution from the field's first N modes.

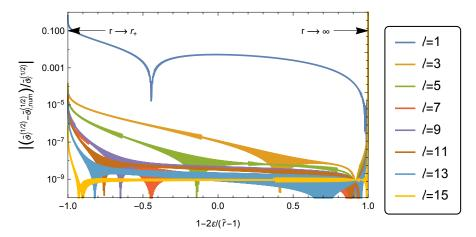


Figure 4. Direct comparison between the analytical solution $\tilde{\vartheta}_{\ell}^{(1/2)}$ and the numerical solution at $a=1-10^{-10}$ (approximately $\varepsilon\approx\sqrt{2}\times10^{-5}$), using the method of [21]. The vertical axis is fractional difference between the numerical solution and the analytical solution for each mode. The extremal solution is evaluated onto the collocation points of the numerical domain $x\in(-1,+1)$ where $x=1-2\varepsilon/(\tilde{r}-1)$. The numerical solution was computed with an angular and radial resolution of $(N_{ang},N_x)=(64,1024)$, and comparisons against lower resolutions shows that the numerics are converging. The limit $\varepsilon\to 0$ is regular, so the fractional differences will go to zero.

the background spacetime, by using the modal contribution to the ADM energy as a proxy. The convergence to the extremal limit is more easily demonstrated by using the extremality parameter as the horizontal axis, as seen in the right panel. We can also

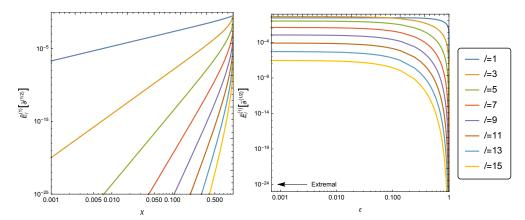


Figure 5. Modal contribution to the ADM energy of the scalar field [defined in Eq. (41)], as a function of rotation on the horizontal axis. Notice that the extremal limit is regular. This is emphasized by making the horizontal axis the extremality parameter $\varepsilon = \sqrt{1-\chi^2}$. Note that each curve becomes horizontal going toward the left edge of the right panel.

easily see that higher ℓ modes become fractionally more important as spin increases (this was seen in Fig. 2 of [21]).

The essential differences between the structure of the scalar field in the slowly rotating $(\chi \to 0)$ and extremal $(\chi \to 1)$ limits are apparent in Fig. 5. At low spin, $\chi \ll 1$, the scalar field is almost entirely dipolar, with contributions to the ADM energy from the $\ell \geq 3$ modes amounting to less than 1 part in 10^{12} . The higher modes become more important as the spin of the background black hole increases, and the octupole contribution to the ADM energy exceeds the dipole contribution at around $\chi \approx 0.995$. At $\chi = 1$, the dipole contributes about 30% of the total ADM energy, while the octupole contributes just over 50%. This is consistent with the near-horizon behavior of the modes shown in Fig. 1, and our earlier observation that the scalar field ADM energy is dominated by the contribution from the near-horizon region.

5. Trace of the Metric Perturbation: Solution

The leading correction to the metric in Eq. (12) is determined by the $\mathcal{O}(\zeta)$ term in the metric equation of motion [Eq. (6)]. We work in a gauge where the covariant divergence of $g_{ab}^{(1)}$ is proportional to the derivative of its trace $g^{(1)} = g_{(0)}^{ab} g_{ab}^{(1)}$ with respect to the background metric:

$$\nabla^a g_{ab}^{(1)} = \frac{1}{2} \nabla_b g^{(1)} \ . \tag{43}$$

This gauge leads to simplifications in the $\mathcal{O}(\zeta)$ term of Eq. (6), but its structure is still too complicated to allow for a simple solution. As a first step towards determining $g_{ab}^{(1)}$, we take the trace of the $\mathcal{O}(\zeta)$ correction to Eq. (6) to find

$$\Box g^{(1)} = -2(\nabla \vartheta^{(1/2)})^2 \ . \tag{44}$$

Assuming a stationary and axisymmetric solution and transforming to dimensionless variables, this reduces to

$$\left[\partial_{\tilde{r}}\tilde{\Delta}\partial_{\tilde{r}} + \partial_{\psi}\Gamma\partial_{\psi}\right]g^{(1)} = -2\tilde{\Delta}(\partial_{\tilde{r}}\tilde{\vartheta}^{(1/2)})^{2} - 2\Gamma(\partial_{\psi}\tilde{\vartheta}^{(1/2)})^{2}. \tag{45}$$

As with the scalar field, we can express $g^{(1)}$ in a Legendre decomposition as

$$g^{(1)} = \sum_{\ell} g_{\ell}^{(1)}(\tilde{r}) P_{\ell}(\psi). \tag{46}$$

Then, the equation of motion [Eq. (45)] again separates, giving the radial equation

$$\left[\partial_{\tilde{r}}\tilde{\Delta}\partial_{\tilde{r}} - \ell(\ell+1)\right]g_{\ell}^{(1)}(\tilde{r}) = S_{\ell}(\tilde{r}). \tag{47}$$

The source functions $S_{\ell}(\tilde{r})$ are the Legendre modes of the right-hand side of Eq. (44), i.e.

$$S_{\ell}(\tilde{r}) = \frac{2\ell + 1}{2} \int_{-1}^{1} d\psi P_{\ell}(\psi) S_{g}(\tilde{r}, \psi) , \qquad (48)$$

where the source function S_q is simply

$$S_q(\tilde{r}, \psi) := -2\sqrt{-g^{(0)}} \left(\nabla \tilde{\vartheta}^{(1/2)}\right)^2.$$
 (49)

The solution for the mode functions $g_{\ell}^{(1)}(\tilde{r})$ is then given by Eq. (A.3), which in this case becomes

$$g_{\ell}^{(1)} = \frac{1}{W_{\ell}} \left(H_{\ell}^{+}(\tilde{r}) \int_{\infty}^{\tilde{r}} d\tilde{r}' H_{\ell}^{-}(\tilde{r}') S_{\ell}(\tilde{r}') - H_{\ell}^{-}(\tilde{r}) \int_{\tilde{r}_{+}}^{\tilde{r}} d\tilde{r}' H_{\ell}^{+}(\tilde{r}') S_{\ell}(\tilde{r}') \right). \tag{50}$$

Note that the source is quadratic in the scalar field, which has odd Legendre modes. Thus, both the trace of the metric perturbation and its source function have even Legendre modes: $\ell = 2n$ for all $n \in \mathbb{N}$.

One approach to evaluating the integrals in Eq. (50) is to express the Legendre modes of the source function in terms of the scalar field modes and their radial derivatives. The resulting integrals are significantly more complicated than the ones we encountered in Sec. 3, so we will opt for a different approach. One can express Eq. (50) in terms of a simpler set of integrals through multiple integrations-by-parts (noting that the source S_{ℓ} depends on S_g , which in turn is proportional to the squared derivative of the scalar field) and application of the scalar field evolution equation [Eq. (20)]. Doing so, the modes of the trace of the metric perturbation are given by

$$g_{\ell}^{(1)}(\tilde{r}) = \frac{2\ell + 1}{W_{\ell}} \left(H_{\ell}^{+}(\tilde{r}) \int_{\infty}^{\tilde{r}} d\tilde{r}' \int_{-1}^{1} d\psi \ H_{\ell}^{-}(\tilde{r}') P_{\ell}(\psi) \tilde{\vartheta}^{(1/2)}(\tilde{r}', \psi) s(\tilde{r}', \psi) - H_{\ell}^{-}(\tilde{r}) \int_{\tilde{r}_{+}}^{\tilde{r}} d\tilde{r}' \int_{-1}^{1} d\psi \ H_{\ell}^{+}(\tilde{r}') P_{\ell}(\psi) \tilde{\vartheta}^{(1/2)}(\tilde{r}', \psi) s(\tilde{r}', \psi) + H_{\ell}^{+}(\tilde{r}) \int_{\infty}^{\tilde{r}} d\tilde{r}' \int_{-1}^{1} d\psi \ \partial_{\mu} V_{-}^{\mu}(\tilde{r}', \psi) - H_{\ell}^{-}(\tilde{r}) \int_{\tilde{r}_{+}}^{\tilde{r}} d\tilde{r}' \int_{-1}^{1} d\psi \ \partial_{\mu} V_{+}^{\mu}(\tilde{r}', \psi) \right) ,$$

$$(51)$$

where $s(\tilde{r}', \psi)$ is the scalar field source given in Eq. (21), and we have defined

$$V_{\pm}^{\mu} := \frac{1}{2} (\tilde{\vartheta}^{(1/2)})^2 \sqrt{-g^{(0)}} g_{(0)}^{\mu\nu} \partial_{\nu} \left[H_{\ell}^{\pm} P_{\ell} \right] - \frac{1}{2} H_{\ell}^{\pm} P_{\ell} \sqrt{-g^{(0)}} g_{(0)}^{\mu\nu} \partial_{\nu} (\tilde{\vartheta}^{(1/2)})^2 . \tag{52}$$

The integrals of total derivatives in Eq. (51) can be simplified by noting that (i) $\sqrt{-g^{(0)}}g_{(0)}^{\psi\psi}=\Gamma$, which vanishes when evaluated at the limits of integration $\psi=\pm 1$, and (ii) contributions at spatial infinity and at the horizon vanish due to the behavior of the scalar field modes $\tilde{\vartheta}^{(1/2)}$, the homogeneous solutions H_{ℓ}^{\pm} , and $\sqrt{-g^{(0)}}g_{(0)}^{rr}=\tilde{\Delta}$. The modes of the trace of the metric perturbation are then

$$g_{\ell}^{(1)}(\tilde{r}) = \frac{2\ell + 1}{W_{\ell}} \left(H_{\ell}^{+}(\tilde{r}) \int_{\infty}^{\tilde{r}} d\tilde{r}' \int_{-1}^{1} d\psi \ H_{\ell}^{-}(\tilde{r}') P_{\ell}(\psi) \tilde{\vartheta}^{(1/2)} s^{(1/2)} \right)$$

$$- H_{\ell}^{-}(\tilde{r}) \int_{\tilde{r}_{+}}^{\tilde{r}} d\tilde{r}' \int_{-1}^{1} d\psi \ H_{\ell}^{+}(\tilde{r}') P_{\ell}(\psi) \tilde{\vartheta}^{(1/2)} s^{(1/2)} \right)$$

$$- \frac{2\ell + 1}{2} \int_{-1}^{1} d\psi \ P_{\ell}(\psi) \left(\tilde{\vartheta}^{(1/2)}(\tilde{r}, \psi) \right)^{2},$$

$$(53)$$

where in the first and second lines $\tilde{\vartheta}^{(1/2)}$ and $s^{(1/2)}$ are both functions of \tilde{r}' and ψ . We have simplified the last line by extracting a factor of W_{ℓ} , defined in Eq. (A.4), which is a constant

Let us now focus on the extremal limit. With the normalizations defined in Appendix A, the factor $W_{\ell} = 2\ell + 1$ and the homogeneous solutions are given by Eqs. (A.8)-(A.9). We can then write

$$g_{\ell}^{(1,0)}(\tilde{r}) = (\tilde{r} - 1)^{\ell} \int_{\infty}^{\tilde{r}} d\tilde{r}' \int_{-1}^{1} d\psi \, \frac{P_{\ell}(\psi)\tilde{\vartheta}^{(1/2,0)} s^{(1/2,0)}}{(\tilde{r} - 1)^{\ell+1}}$$

$$- \frac{1}{(\tilde{r} - 1)^{\ell+1}} \int_{1}^{\tilde{r}} d\tilde{r}' \int_{-1}^{1} d\psi \, (\tilde{r} - 1)^{\ell} P_{\ell}(\psi) \tilde{\vartheta}^{(1/2,0)} s^{(1/2,0)}$$

$$- \frac{(2\ell+1)}{2} \int_{-1}^{1} d\psi P_{\ell}(\psi) \, (\tilde{\vartheta}^{(1/2,0)})^{2} \, . \tag{54}$$

This completes the formal solution for the modes of the trace of the metric perturbation in the extremal limit in integral form.

The angular integrals in Eq. (54) can be evaluated in closed form using the Legendre decomposition of the scalar field and the source function. From Eq. (22) and Eq. (24) we have

$$\tilde{\vartheta}^{(1/2,\,0)}(\tilde{r},\psi) = \sum_{k=1}^{\infty} \tilde{\vartheta}_{k}^{(1/2,\,0)}(\tilde{r}) P_{k}(\psi)$$
$$s^{(1/2,\,0)}(\tilde{r},\psi) = \sum_{j=1}^{\infty} s_{j}^{(1/2,\,0)}(\tilde{r}) P_{j}(\psi),$$

where the sums are over odd integers in both cases. Using the orthogonality of Legendre

functions, the $\ell = 0$ mode is given by

$$g_0^{(1,0)}(\tilde{r}) = \sum_{k=1}^{\infty} \frac{2}{2k+1} \left[\int_{\infty}^{\tilde{r}} d\tilde{r}' \frac{\tilde{\vartheta}_k^{(1/2,0)}(\tilde{r}') s_k^{(1/2,0)}(\tilde{r}')}{\tilde{r}'-1} - \frac{1}{\tilde{r}-1} \int_{1}^{\tilde{r}} d\tilde{r}' \, \tilde{\vartheta}_k^{(1/2,0)}(\tilde{r}') s_k^{(1/2,0)}(\tilde{r}') - \frac{1}{2} \, \tilde{\vartheta}_k^{(1/2,0)}(\tilde{r})^2 \right]. \tag{55}$$

For general ℓ , the integration over ψ can be expressed in terms of the standard 3j-symbols. The resulting expression is

$$g_{\ell}^{(1,0)}(\tilde{r}) = \sum_{k,j} 2 \begin{pmatrix} \ell & k & j \\ 0 & 0 & 0 \end{pmatrix}^{2} \times \left[(\tilde{r} - 1)^{\ell} \int_{\infty}^{\tilde{r}} d\tilde{r}' \frac{\tilde{\vartheta}_{k}^{(1/2,0)}(\tilde{r}') s_{j}^{(1/2,0)}(\tilde{r}')}{(\tilde{r}' - 1)^{\ell+1}} \right]$$

$$- \frac{1}{(\tilde{r} - 1)^{\ell+1}} \int_{1}^{\tilde{r}} d\tilde{r}' (\tilde{r}' - 1)^{\ell} \tilde{\vartheta}_{k}^{(1/2,0)}(\tilde{r}') s_{j}^{(1/2,0)}(\tilde{r}')$$

$$- \frac{2\ell + 1}{2} \tilde{\vartheta}_{k}^{(1/2,0)}(\tilde{r}) \tilde{\vartheta}_{j}^{(1/2,0)}(\tilde{r})$$

$$(56)$$

The radial integrals in Eqs. (55) and (56), though still complicated, are more tractable than the integrals that result from expressing the source function in terms of the modes of the scalar field in Eq. (50).

We have not yet obtained a closed-form expression for the trace of the metric perturbation on the extremal background. The main difficulty, apparent in Eqs. (54)-(56), is that the source term depends on the full tower of Legendre modes of the scalar field. Using our expressions for the modes of the scalar field and its source, Eq. (33) and Eq. (25), it is possible to evaluate individual terms in these sums. However, we have not been able to perform the sums themselves. Indeed, the analytic results for the individual terms are sufficiently complicated that we turn to approximations and numerical analysis, which we discuss in the next section.

6. Trace of the Metric Perturbation: Properties

The results of Sec. 4 suggest that the first three or four modes of the scalar field capture most of its physics, and should be sufficient for analyzing the behavior of the trace of the metric perturbation. But first, let us consider a few important properties of the modes $g_{\ell}^{(1,0)}$ that can be extracted from the integral form of the solution.

At large radius, $\tilde{r} \gg 1$, the second line of Eq. (54) dominates and the leading behavior of the mode is $g_{\ell}^{(1,0)} \sim \tilde{r}^{-(\ell+1)}$. This is because the first line of Eq. (54) decays with a higher power of \tilde{r} , while the third line is proportional to $(\tilde{\vartheta}^{(1/2,0)})^2$ and therefore decays as $\tilde{r}^{-2(\ell+1)}$. Near the horizon the first and third line of Eq. (54) dominate. The asymptotic behavior as $\tilde{r} \to 1$ is most easily extracted by first evaluating Eq. (50) at $\tilde{r} = \tilde{r}_+ = 1 + \varepsilon$, changing the integration variable to $\eta = (\tilde{r}' - 1)/\varepsilon$, and then taking the $\varepsilon \to 0$ limit, which gives

$$g_{\ell}^{(1,0)}(1) = S_{\ell}^{(1,0)}(1) \int_{\infty}^{1} d\eta \, Q_{\ell}(\eta) . \tag{57}$$

The overall factor of $S_{\ell}^{(1,0)}(1)$, the source function evaluated at the extremal Kerr horizon, can be expressed in terms of the source functions for the scalar field. Evaluating

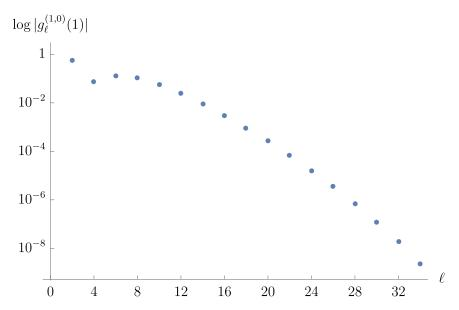


Figure 6. The (absolute value of) Legendre modes of the trace of the metric perturbation evaluated at the horizon of the extremal background, on a logarithmic scale, as a function of harmonic number ℓ .

Eq. (48) at $\tilde{r} = 1$, using $\lim_{\tilde{r} \to 1} \tilde{\Delta}(\partial_{\tilde{r}}\tilde{\vartheta})^2 = 0$, and performing the angular integral yields

$$S_{\ell}^{(1,0)}(1) = -\sum_{k,j=1}^{\infty} \frac{2(2\ell+1)}{\sqrt{j(j+1)k(k+1)}} \begin{pmatrix} \ell & j & k \\ 0 & 0 & 0 \end{pmatrix} \begin{pmatrix} \ell & j & k \\ 0 & 1 & -1 \end{pmatrix} s_{j}^{(1/2,0)}(1) s_{k}^{(1/2,0)}(1) ,$$

$$(58)$$

where again the result is expressed in terms of 3i-symbols.

For $\ell \geq 2$ (recall that ℓ is even) the integral in Eq. (57) converges:

$$g_{\ell}^{(1,0)}(1) = -\frac{1}{\ell(\ell+1)} S_{\ell}^{(1,0)}(1) . \tag{59}$$

In this case the mode is finite at the horizon of the extremal background, just like the modes of the scalar field. The values $g_{\ell}^{(1,0)}(1)$ are plotted against ℓ in Fig. 6. Rather than falling off monotonically with ℓ , a feature is observed at $\ell=4$. This mode is suppressed relative to the $\ell=6$ and $\ell=8$ modes.

For the $\ell=0$ mode the integral in Eq. (57) does not converge. In this case the mode diverges logarithmically as $\tilde{r}\to 1$. Its behavior near the horizon is captured by the first integral in Eq. (55). Expanding the integrand in powers of $(\tilde{r}'-1)$ and extracting the log term from the integral gives

$$\lim_{\tilde{s} \to 1} g_0^{(1,0)}(\tilde{r}) \sim S_0^{(1,0)}(1) \log(\tilde{r} - 1) , \qquad (60)$$

The coefficient $S_0^{(1,0)}(1)$ may be evaluated from Eq. (58), which for $\ell=0$ reduces to a

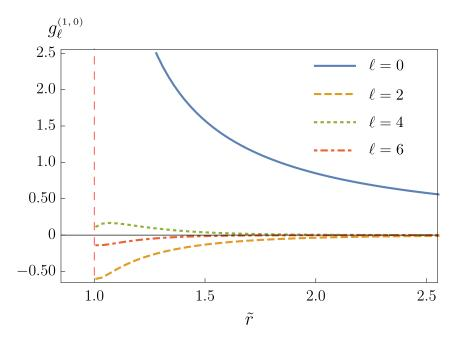


Figure 7. The first four radial modes of the trace of the metric perturbation as a function of \tilde{r} . The dashed vertical line indicates the horizon of the extremal background. The $\ell=0$ mode exhibits a logarithmic divergence as $\tilde{r}\to 1$.

single sum

$$S_0^{(1,0)}(1) = -\sum_{k=1}^{\infty} \frac{2}{k(k+1)(2k+1)} \left(s_k^{(1/2,0)}(1)\right)^2$$

$$\sim -3.52572.$$
(61)

This is the same value that is obtained from the ratio of the numerical solution for $g_0^{(1,0)}(\tilde{r})$ and $\log(\tilde{r}-1)$, evaluated as $\tilde{r}\to 1$. As we will discuss at the end of this Section, the log divergence in $g_0^{(1,0)}(\tilde{r})$ need not imply the existence of a naked curvature singularity at the perturbed horizon.

As explained at the end of the previous Section, analytical results for the \tilde{r} -dependence of the modes $g_{\ell}^{(1,0)}$ are sufficiently complicated that a numerical analysis is called for. The first four modes of the trace of the metric perturbation are shown in Fig. 7. These are numerical solutions, obtained with closed form expressions for the source that include contributions from modes of the scalar field with $\ell \leq 21$. It is immediately apparent that the $\ell = 0$ mode dominates the trace of the metric perturbation, even away from the log-divergent behavior near $\tilde{r} = 1$.

We expect, based on the behavior shown in Fig. 7 that $g^{(1,0)}$ is well-approximated by its first few Legendre modes. In the case of the scalar field, a similar conclusion was justified by examining mode-by-mode contributions to the ADM energy. But before applying this norm to the modes of the trace of the metric perturbation, we first consider the fractional difference between $g^{(1,0)}(\tilde{r},\psi)$ evaluated at $\psi=1$, and an

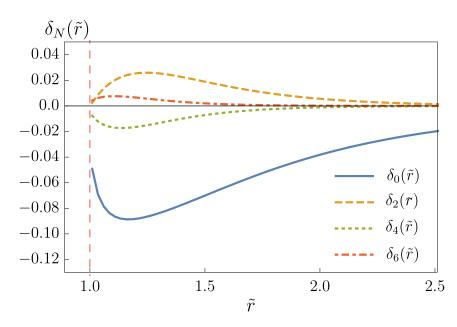


Figure 8. The fractional difference between the trace of the metric perturbation at $\theta = 0$, and its approximation including only modes with $\ell \leq N$.

approximation by its first N modes

$$\delta_N(\tilde{r}) = 1 - \frac{1}{g^{(1,0)}(\tilde{r},1)} \left(\sum_{\ell=0}^N g_{\ell}^{(1,0)}(\tilde{r}) \right) . \tag{62}$$

The fractional difference for N=0,2,4,6 is shown in Fig. 8. As expected, the log-divergence of the $\ell=0$ modes means that the fractional difference $\delta_0(\tilde{r})\to 0$ as $\tilde{r}\to 1$. Figure 8 shows that if one wishes an accuracy of no more than about 10%, then retaining only the $\ell=0$ mode suffices. To obtain a higher accuracy, more modes are needed. In particular, since the $\ell=4$ mode is suppressed at $\tilde{r}=1$ relative to the $\ell=6$ and 8 modes, one must include modes up to $\ell=6$ to obtain uniform accuracy of at least one percent. Observe, however, that if one is interested in the trace of the metric perturbation outside a larger radius, such as for $\tilde{r}\gtrsim 2$, then $g^{(1,0)}$ is approximated at better than percent precision with only the first two or three modes.

We conclude that Legendre modes $g_{\ell}^{(1,0)}$ with $\ell \leq 4$ capture almost all of the physics of $g^{(1,0)}$, except near $\tilde{r}=1$ where the $\ell=6$ and $\ell=8$ modes may be required. Note that the fractional error defined in Eq. (62) puts a bound on the fidelity of our approximation of $g^{(1,0)}$ at $\psi=1$ ($\theta=0$), where $P_{\ell}(\psi)=1$ for all ℓ . However, since the $\ell=0$ mode dominates, and $-1 \leq P_{\ell}(\psi) \leq 1$ for $\ell \geq 2$, the fractional error $\delta_N(\tilde{r})$ gives an upper bound on the fidelity of the approximation in the full (\tilde{r},ψ) plane. An approximation of $g^{(1,0)}$ by its first four Legendre modes is shown in Fig. 9.

The analysis above uses modes of the scalar field with $\ell \leq 21$ to approximate the source for the trace of the metric perturbation. However, as we saw in Sec. 4, the first three modes of the scalar field account for most of its contribution to the ADM energy. Indeed, the behavior of the first few modes of $g^{(1,0)}$ is largely unchanged if we include fewer modes of the scalar field. In particular, we achieve comparable results for the

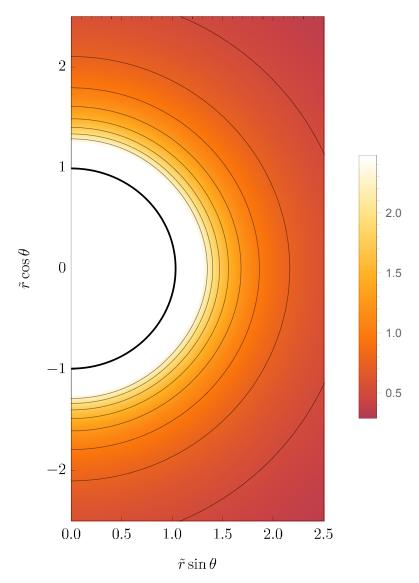


Figure 9. The trace of the metric perturbation on the extremal background, approximated by its first four Legendre modes. Near the extremal horizon $\tilde{r}=1$ (the solid line) the logarithmic divergence of the monopole term dominates.

mode $g_{\ell}^{\scriptscriptstyle (1,\,0)}$ by approximating the scalar field by its first $N=\ell+1$ modes.

Just as in the case of the scalar field, we can study the convergence of numerical solutions with $\varepsilon>0$ in the limit as $\varepsilon\to 0$, using the numerical technique of Stein [21]. We use the ADM energy functional, given in Eq. (41), as a norm for the modes $g_\ell^{(1)}$. Despite the fact that $g_0^{(1)}$ has a logarithmic divergence at the horizon, this divergence is integrable in the norm of Eq. (41). This results in each of the ℓ modes' energies being convergent as $\varepsilon\to 0$, as seen in Fig. 10.

As in Sec. 4, we can again plainly see the differences between the trace of the

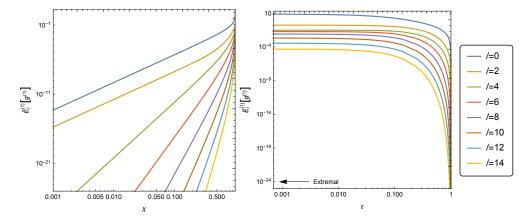


Figure 10. Using the scalar ADM energy functional [defined in Eq. (41)] to measure the contributions to the trace of the metric perturbation $g^{(1)}$ in each ℓ mode. Notice that the modal energy in the extremal limit is regular, despite the logarithmic divergence in the $\ell=0$ mode. This is emphasized by making the horizontal axis the extremality parameter $\varepsilon=\sqrt{1-\chi^2}$. Note that each curve becomes horizontal going toward the left edge of the right panel.

metric perturbation in the slowly rotating and extremal limits, with the higher ℓ modes becoming fractionally more important as rotation increases. In the slowly rotating case the monopole mode dominates, with the energy of the modes falling off like $\chi \ll 1$ to a power that is monotonically increasing with ℓ . For χ sufficiently close to zero, the monopole and quadrupole modes of the trace of the metric perturbation account for the ADM energy to better than 1 part in 10^{12} . Near extremality, the monopole mode still dominates, but the contributions to the ADM energy from the first eight modes ($\ell \leq 14$) span a range of only about 8 decades. As pointed out earlier, approximating the trace of the metric perturbation to better than 1% fidelity in the extremal limit requires at least the first four modes ($\ell \leq 6$). Thus, as with the scalar field, modes of the trace of the metric perturbation that are not relevant in the limit of slow rotation become more important near extremality.

Finally, we turn to the question of the significance of the logarithmic divergence of the $\ell=0$ mode, as seen in Eq. (60). Without a full metric tensor perturbation solution, we cannot determine if this is a true curvature singularity of the perturbed spacetime. However, several pieces of evidence suggest that a divergence in the trace of the metric perturbation need not be a problem.

First, note that shifts within the Kerr family of solutions manifest perturbatively as divergences of the trace of the metric perturbation. Consider shifting the Kerr metric by $M \to M + \delta M$ and $a \to a + \delta a$, and expanding the resulting metric in powers of $\delta M \ll M$ and $\delta a \ll a$. This is made formal by the coefficients in the Taylor series, which are given by

$$(\delta_M g)_{ab} \equiv \frac{\partial}{\partial M} g_{ab} \,, \qquad (\delta_a g)_{ab} \equiv \frac{\partial}{\partial a} g_{ab} \,, \qquad (63)$$

and so on for higher derivatives, e.g. $\delta_{M,M}g_{ab}$. The perturbed shifted Kerr metric tensor satisfies the perturbative Einstein equations order-by-order, since they are simply shifts of the Kerr parameters M and a. A straightforward calculation in Boyer-Lindquist

coordinates, however, shows that

$$\operatorname{Tr}[\delta_M g] = 0, \qquad \operatorname{Tr}[\delta_a g] = \frac{4a\cos^2\theta}{\Sigma},$$
 (64)

$$\operatorname{Tr}[\delta_{M}g] = 0, \qquad \operatorname{Tr}[\delta_{a}g] = \frac{4a\cos^{2}\theta}{\Sigma}, \qquad (64)$$

$$\operatorname{Tr}[\delta_{M,M}g] = \frac{8r^{2}}{\Delta^{2}}, \qquad \operatorname{Tr}[\delta_{a,M}g] = \frac{p_{1}(r,\cos\theta)}{\Delta^{2}\Sigma}, \qquad \operatorname{Tr}[\delta_{a,a}g] = \frac{p_{2}(r,\cos\theta)}{\Delta^{2}\Sigma^{2}}, \qquad (65)$$

where $p_{1,2}$ are certain regular polynomials of r and $\cos \theta$, neither of which have zeros at the roots of either Δ or Σ . Although the Kerr spacetime is regular, as are the linearly or quadratically shifted spacetimes, we immediately see that the traces of the above metric perturbations diverge at either the event and Cauchy horizons where $\Delta = 0$, or the (ring) curvature singularity where $\Sigma = 0$, or both. Only the blowup at the curvature singularity can be seen as physically significant. When $a \to M$, in Boyer-Lindquist coordinates, the curvature singularity appears on the horizon, at the equator.

Next we can bring in arguments that are more specific to the dCS problem. As noted by Stein [21], the (inner) Cauchy-horizon divergence of the scalar found by Konno and Takahashi [20] may result in a divergence of the trace of the metric perturbation at the inner horizon; however, this divergence would be hidden by the outer horizon for all |a| < M. Indeed, Ref. [21], found that the trace of the metric perturbation is regular in the exterior for all |a| < M. However, in the limit $a \to M$, the inner and outer horizons confluence. Further, in the slow-rotation expansion, the horizon was seen to be shifted outward to $r_{\text{hor}} = r_{\text{hor,Kerr}} + (915/28672)\zeta M\chi^2 + \mathcal{O}(\chi^4)$ [19]. Thus, one may expect that in the extremal limit, the perturbed horizon may again be exterior to that of the background, hiding any potential singularity. Finally, it may be the case that the extremality condition in dCS is shifted away from $J = M^2$.

All of these arguments suggest that the horizon singularity in $g_0^{(1,0)}$ may not be a physical curvature singularity, but rather a coordinate singularity. A full tensor perturbation solution is needed to confirm this conjecture.

7. Discussion

This paper explored rotating black holes in dCS. Using an effective field theory treatment of dCS, we worked in the decoupling limit where dCS corrections are small perturbations from GR solutions. We have further focused on BHs that spin at the maximal Kerr rate, the so-called extremal limit. With these assumptions, we then solved for the dynamical scalar field in closed analytic form, obtaining a Legendre decomposition that is dominated by its dipole and octupole terms. The radial structure of this decomposition includes natural logarithms and arctangents, unlike the simple polynomial results obtained in the slow-rotation limit. We then solved for the Legendre decomposition of the trace of the metric perturbation. Retaining Legendre modes with $\ell \leq 6$ is sufficient to ensure a fidelity of at least 99% relative to numerical solutions for both the scalar field and the trace of the metric perturbation.

The trace of the metric perturbation in the Lorenz-like gauge exhibits a logarithmic divergence at the location of the background (extremal Kerr) event horizon. Several pieces of evidence, discussed in Sec. 6, show that it need not be a physical curvature singularity. We conjecture that it is only a coordinate singularity, but a full metric tensor perturbation solution is needed to confirm this conjecture.

The techniques we employed rely heavily on Legendre expansions, but our work suggests that these can be truncated at a finite mode number without losing much of

the overall behavior of the fields. In particular, if one wishes to carry out astrophysical tests of GR, certain observables may be sensitive to only certain regions of spacetime that need not include the horizon. For example, BH shadow observations are most sensitive to the location of the light-ring, while astrophysical observations of the energy spectrum of radiation emitted by accretion disks are most sensitive to the location of the innermost stable circular orbit. For such observations, it may suffice to keep only the first few modes in a Legendre expansion provided the BH is not rotating maximally. The reason here is two-fold. First, the light-ring and ISCO are both pushed away from the horizon as the spin decreases, and the approximation by a finite number of Legendre modes improves away from the immediate vicinity of the horizon. Second, our studies indicate that, in general, the fidelity of an approximation with a fixed number of modes improves away from extremality, as shown in [21].

The results obtained here open the door for new investigations of rotating BHs in dCS gravity. As mentioned in the introduction, the methods we employed can be applied to the next-order term in a near-extremal expansion. They also generalize to BHs that rotate with arbitrary spins, and we have already obtained closed-form results in that case for the first few modes of the scalar field (and numerical results for all other modes). Ultimately, of course, our goal is to go beyond the trace and determine the full metric perturbation of dCS BHs. Previous work on this problem was limited by incomplete results for the scalar field, but with the results in this paper we are now in a position to attack the full problem.

Acknowledgments

We would like to thank the Kavli Institute for Theoretical Physics for their hospitality during the completion of this work. We would also like to thank Kent Yagi, Frans Pretorius, and Albion Lawrence for useful discussions. RM acknowledges support from a Loyola University Chicago Summer Research Stipend. LCS acknowledges that support for this work was provided by NASA through Einstein Postdoctoral Fellowship Award Number PF2-130101 issued by the Chandra X-ray Observatory Center, which is operated by the Smithsonian Astrophysical Observatory for and on behalf of the NASA under contract NAS8-03060, and further acknowledges support from the NSF grant PHY-1404569. NY acknowledges support from NSF CAREER Award PHY-1250636. The research of RM and NY was supported in part by the National Science Foundation under Grant No. NSF PHY11-25915. Some calculations used the computer algebra-system Maple, in combination with the GRTensorII package [48]. Other calculations used the computer algebra-system MATHEMATICA, in combination with the XTENSOR package [49, 50, 51]. Finally, RM (@mcnees) and LCS (Qduetosymmetry) would like to thank Twitter for facilitating discussion during the early stages of this collaboration.

Appendix A. Solution of the Scalar Equation of Motion

The equations of motion for the scalar field and the trace of the metric perturbation have the same general form, so let us briefly establish some conventions for the solutions of such equations. First, consider an equation of the form

$$\partial_{\tilde{r}}(\tilde{\Delta}\partial_{\tilde{r}}I_{\ell}) - \ell(\ell+1)I_{\ell} = K_{\ell} \tag{A.1}$$

with some source K_{ℓ} . Denote by H_{ℓ}^+ and H_{ℓ}^- the solutions of the homogeneous equation

$$\partial_{\tilde{r}}(\tilde{\Delta}\partial_{\tilde{r}}H_{\ell}^{\pm}) - \ell(\ell+1)H_{\ell}^{\pm} = 0, \qquad (A.2)$$

with H_{ℓ}^+ regular at \tilde{r}_+ and $H_{\ell}^- \to 0$ at $\tilde{r} \to \infty$. We use the method of variation of parameters to find the general solution to the inhomogeneous equation. The solution of (A.1) that is both regular at \tilde{r}_+ and goes to zero as $\tilde{r} \to \infty$ can be expressed in terms of the homogeneous solutions and the source as

$$I_{\ell} = \frac{1}{W_{\ell}} \times \left(H_{\ell}^{+}(\tilde{r}) \int_{\infty}^{\tilde{r}} d\tilde{r}' H_{\ell}^{-}(\tilde{r}') K_{\ell}(\tilde{r}') - H_{\ell}^{-}(\tilde{r}) \int_{\tilde{r}_{+}}^{\tilde{r}} d\tilde{r}' H_{\ell}^{+}(\tilde{r}') K_{\ell}(\tilde{r}') \right) . \quad (A.3)$$

Here a factor of $\tilde{\Delta}$ has canceled inside each integral, allowing us to pull out a constant W_{ℓ} ; this constant depends on the Wronskian of the homogeneous solutions,

$$W_{\ell} \equiv \tilde{\Delta} \times W[H_{\ell}^{-}, H_{\ell}^{+}]$$

$$= \tilde{\Delta} \times (H_{\ell}^{-} \partial_{\tilde{r}} H_{\ell}^{+} - H_{\ell}^{+} \partial_{\tilde{r}} H_{\ell}^{-}) . \tag{A.4}$$

It is straightforward to verify that this is constant using Eq. (A.2).

For the Kerr background, the homogeneous solutions can be written as

$$H_{\ell}^{+}(\tilde{r}) = c_{\ell}^{+} (1 - \chi^{2})^{\frac{\ell}{2}} P_{\ell} \left(\frac{\tilde{r} - 1}{\sqrt{1 - \chi^{2}}} \right)$$
(A.5)

$$H_{\ell}^{-}(\tilde{r}) = c_{\ell}^{-} (1 - \chi^{2})^{-\frac{\ell+1}{2}} Q_{\ell} \left(\frac{\tilde{r} - 1}{\sqrt{1 - \chi^{2}}} \right) .$$
 (A.6)

where $P_{\ell}(\cdot)$ and $Q_{\ell}(\cdot)$ are Legendre functions of the first and second kind, respectively. A standard identity for Legendre functions then gives the factor $W_{\ell} = c_{\ell}^{+} c_{\ell}^{-}$.

The factors of $\sqrt{1-\chi^2}$ in Eq. (A.5)-(A.6) have been chosen so that the extremal limit, $\chi \to \pm 1$, is regular. Otherwise, the overall normalization factors c_ℓ^{\pm} are arbitrary. A convenient choice is to set

$$c_{\ell}^{+} = \frac{\ell!}{(2\ell-1)!!}, \qquad c_{\ell}^{-} = \frac{(2\ell+1)!!}{\ell!}.$$
 (A.7)

Then $W_{\ell} = 2\ell + 1$, and in the extremal limit the homogeneous solutions are simply

$$\lim_{|\chi| \to 1} H_{\ell}^{+} = (\tilde{r} - 1)^{\ell} \tag{A.8}$$

$$\lim_{|\chi| \to 1} H_{\ell}^{-} = \frac{1}{(\tilde{r} - 1)^{\ell + 1}} . \tag{A.9}$$

We adopt this normalization throughout Secs. 3 and 5.

Appendix B. Expressions for Radial Modes

The radial mode function for general ℓ is given in Eq. (33). In this form, each mode depends on $2\ell + 1$ coefficients $\alpha_{\ell,k}$ and $\beta_{\ell,k}$. The coefficients for the modes up to $\ell = 9$ are given below.

k	$\alpha_{1,k}$	$\beta_{1,k}$	$\alpha_{3,k}$	$\beta_{3,k}$	$\alpha_{5,k}$	$\beta_{5,k}$	$\alpha_{7,k}$	$\beta_{7,k}$	$\alpha_{9,k}$	$\beta_{9,k}$
0	0	-3	190 3	$\frac{15}{2}$	$-\frac{68}{5}$	$-\frac{85}{8}$	$\frac{31719}{70}$	$\frac{189}{16}$	$\frac{49019}{1260}$	$-\frac{1377}{128}$
1	-	3	-55	-75	$\frac{1015}{8}$	$\frac{2955}{8}$	$-\frac{22317}{80}$	$-\frac{4347}{4}$	$\frac{351417}{896}$	$\frac{315405}{128}$
2	-	-	15	75	$-\frac{8645}{8}$	$-\frac{735}{2}$	$\frac{90819}{20}$	$\frac{8127}{8}$	$-\frac{13832005}{896}$	$-\frac{34155}{16}$
3	-	-	-	-25	$\frac{4263}{8}$	$\frac{4935}{4}$	$-\frac{44079}{16}$	$-\tfrac{33705}{4}$	$\frac{3351161}{384}$	$\frac{1065405}{32}$
4	_	-	_	-	$-\frac{819}{8}$	$-\frac{4935}{8}$	$\frac{21009}{2}$	$\frac{73395}{16}$	$-\frac{9069467}{128}$	$-\frac{1183545}{64}$
5	_	-	_	-	-	$\frac{987}{8}$	$-\tfrac{14067}{4}$	$-\tfrac{44793}{4}$	$\frac{3456585}{128}$	$\frac{6416487}{64}$
6	_	-	_	-	-	-	$\frac{1989}{4}$	$\frac{14931}{4}$	$-\frac{30089455}{384}$	$-\frac{292215}{8}$
7	_	-	_	-	-	-	-	$-\frac{2133}{4}$	$\frac{2523125}{128}$	$\frac{2579445}{32}$
8	_	-	_	-	-	-	-	-	$-\frac{279565}{128}$	$-\frac{2579445}{128}$
9	_	-	-	-	-	-	-	-	-	$\frac{286605}{128}$

Appendix C. Representations of the Scalar Field

Equation (33) provides one representation of the solution to Eq. (23) for arbitrary harmonic number ℓ after a Legendre decomposition and in an expansion to leading order in ζ (i.e. in the GR deformation) and in ε (i.e., in the extremal limit). This form of the solution depends on $2\ell + 1$ coefficients ($\alpha_{\ell,k}$ and $\beta_{\ell,k}$) that are fixed by imposing appropriate boundary conditions on the mode.

In this appendix, we present two additional representations of the solution to the scalar field evolution equation that may be preferable in some applications. As in the case of Eq. (33), these representations will have both advantages and disadvantages that we will describe in detail. The solutions start by representing the source function in the extremal limit in terms of a series:

$$s_{\ell}^{(1/2,0)}(\tilde{r}) = \sum_{n=0}^{\infty} \alpha_{\ell,n} \frac{2\ell+1}{\tilde{r}^{\ell+4+2n}} , \qquad (C.1)$$

where we have introduced the constants

$$\alpha_{\ell,n} = (-1)^{\frac{\ell-1}{2}} (-1)^n \frac{(\ell+2n+2)\Gamma(\ell+4+2n)\Gamma(\frac{1}{2})}{2^{\ell+1+2n}\Gamma(n+1)\Gamma(\ell+n+\frac{3}{2})} , \qquad (C.2)$$

in terms of the Gamma function $\Gamma(\cdot)$. The factor of $2\ell + 1$ in Eq. (C.1) has been introduced to simplify some expressions, by canceling a similar factor in the denominator of Eq. (28). From here on, different representations take different routes to arrive at a solution to Eq. (23) in the extremal limit, so we tackle each of them separately below.

Appendix C.1. Incomplete Beta Function Representation

Introducing expansion Eq. (C.1) for the scalar source into the solution Eq. (28) for the scalar field:

$$\tilde{\vartheta}_{\ell}^{(1/2,0)}(\tilde{r}) = \sum_{n=0}^{\infty} \alpha_{\ell,n} \left[(\tilde{r} - 1)^{\ell} \int_{\infty}^{\tilde{r}} \frac{d\tilde{r}'}{(\tilde{r}' - 1)^{\ell+1} \tilde{r}'^{\ell+4+2n}} - \frac{1}{(\tilde{r} - 1)^{\ell+1}} \int_{1}^{\tilde{r}} d\tilde{r}' (\tilde{r}' - 1)^{\ell} \frac{1}{\tilde{r}'^{\ell+4+2n}} \right], \quad (C.3)$$

where we have already imposed appropriate boundary conditions. The integrals can be evaluated in closed-form to obtain

$$\tilde{\vartheta}_{\ell}^{(1/2,0)}(\tilde{r}) = \beta_1(\tilde{r}) + \beta_2(\tilde{r}) + \beta_3(\tilde{r}) \tag{C.4}$$

where we have defined

$$\beta_1(\tilde{r}) = -\sum_{n=0}^{\infty} \alpha_{\ell,n} (\tilde{r} - 1)^{\ell} B_{1/\tilde{r}} \left(2\ell + 4 + 2n, -\ell \right), \tag{C.5}$$

$$\beta_2(\tilde{r}) = \sum_{n=0}^{\infty} \frac{\alpha_{\ell,n}}{(\tilde{r}-1)^{\ell+1}} B_{1/\tilde{r}} \left(2n+3, \ell+1 \right), \tag{C.6}$$

$$\beta_3(\tilde{r}) = -\sum_{n=0}^{\infty} \frac{\alpha_{\ell,n}}{(\tilde{r}-1)^{\ell+1}} \frac{\Gamma(\ell+1)\Gamma(2n+3)}{\Gamma(\ell+4+2n)}, \tag{C.7}$$

in terms of the incomplete Beta function $B_x(a,b)$ (see e.g. Sec. 8.17 of [52]),

$$B_x(a,b) \equiv \int_0^x t^{a-1} (1-t)^{b-1} dt$$
. (C.8)

Evaluating at x = 1 gives the ordinary Beta function, $B(a, b) = B_1(a, b)$.

The sums over n can be evaluated in closed form for β_2 and β_3 . The latter can be summed into

$$\beta_3(\tilde{r}) = \frac{(-1)^{\frac{\ell+1}{2}} \ell \Gamma(\ell+1)\Gamma(\frac{1}{2})}{2^{\ell+2}\Gamma(\ell+\frac{3}{2})} \frac{1}{(\tilde{r}-1)^{\ell+1}} \left[\ell (2\ell+1) - 2(\ell-1)(\ell+1)_2 F_1(-\frac{1}{2}, 1; \ell+\frac{3}{2}; -1) \right], \quad (C.9)$$

which gives the leading behavior of $\tilde{\vartheta}_{\ell}^{(1/2,0)}$ at large \tilde{r} . The sum over n for β_2 can be evaluated using the series representation of the incomplete Beta function appropriate for Eq. (C.6),

$$B_x(m,n) = \sum_{j=0}^{n-1} \frac{(-1)^j}{m+j} \frac{\Gamma(n)}{\Gamma(j+1)\Gamma(n-j)} x^{m+j} .$$
 (C.10)

Permuting the order of the sums over j and n yields

$$\beta_{2}(\tilde{r}) = \frac{(-1)^{(\ell+3)/2}\Gamma(\ell+1)\Gamma(1/2)\Gamma(4+\ell)}{2^{2+\ell}\Gamma(5/2+\ell)(\tilde{r}-1)^{\ell+1}} \sum_{j=0}^{\ell} \frac{(-1)^{j}}{(3+j)(5+j)} \frac{1}{\Gamma(1+j)\Gamma(1+\ell-j)} \frac{1}{\tilde{r}^{5+j}} \times \left[(5+j)(2+\ell)(3+2\ell) \ \tilde{r}^{2} \ _{3}F_{2}\left(\frac{3+j}{2}, \frac{4+\ell}{2}, \frac{5+\ell}{2}; \frac{5+j}{2}, \frac{3+2\ell}{2}; -\frac{1}{\tilde{r}^{2}}\right) \right] - (3+j)(4+\ell)(5+\ell) \ _{3}F_{2}\left(\frac{5+j}{2}, \frac{6+\ell}{2}, \frac{7+\ell}{2}; \frac{7+j}{2}, \frac{5+2\ell}{2}; -\frac{1}{\tilde{r}^{2}}\right) \right], (C.11)$$

where ${}_{P}F_{Q}(\cdot;\cdot;\cdot)$ is the generalized hypergeometric function. We have not succeeded in finding a closed-form expression for the above sum over j, but the sum can be performed explicitly given any value of ℓ .

One is then only left with the sum over n for β_1 . To obtain an expression for this sum, we start with the following representation of the incomplete Beta function relevant for Eq. (C.5):

$$\begin{split} B_{\frac{1}{\tilde{r}}}\left(2\ell+4+2n,-\ell\right) &= \frac{(-1)^{\ell+1}(\ell+4+2n)\Gamma(2\ell+4+2n)}{\Gamma(\ell+1)\Gamma(\ell+5+2n)} \times \left[\ln\left(\frac{\tilde{r}-1}{\tilde{r}}\right)\right. \\ &\left. + \frac{1}{\tilde{r}-1}\left(1-\sum_{k=1}^{\ell+3+2n}\frac{1}{k(k+1)}\frac{1}{\tilde{r}^k}\right)\right] \\ &\left. - \frac{\Gamma(2\ell+4+2n)}{\Gamma(\ell+1)}\frac{1}{\tilde{r}^{\ell+3+2n}}\sum_{k=0}^{\ell-2}(\tilde{r}-1)^{k-\ell}\frac{(-1)^{k+1}\Gamma(\ell-k)}{\Gamma(2\ell+4+2n-k)}\right. \end{split}$$
 (C.12)

This allows us to write $\beta_1(\tilde{r}) := \beta_4(\tilde{r}) + \beta_5(\tilde{r})$, where we have defined

$$\beta_4(\tilde{r}) = -(\tilde{r} - 1)^{\ell} \sum_{n=0}^{\infty} \alpha_{\ell,n} \frac{(-1)^{\ell+1} (\ell + 4 + 2n) \Gamma(2\ell + 4 + 2n)}{\Gamma(\ell + 1) \Gamma(\ell + 5 + 2n)} \times \left[\ln \left(\frac{\tilde{r} - 1}{\tilde{r}} \right) + \frac{1}{\tilde{r} - 1} \left(1 - \sum_{k=1}^{\ell+3+2n} \frac{1}{k(k+1)} \frac{1}{\tilde{r}^k} \right) \right]$$
(C.13)

$$\beta_5(\tilde{r}) = -\frac{1}{\Gamma(\ell+1)} \frac{1}{\tilde{r}^{\ell+3}} \sum_{n=0}^{\infty} \alpha_{\ell,n} \frac{\Gamma(2\ell+4+2n)}{\tilde{r}^{2n}} \sum_{k=0}^{\ell-2} \frac{(-1)^k \Gamma(\ell-k)}{\Gamma(2\ell+4+2n-k)} (\tilde{r}-1)^k.$$
(C.14)

The function $\beta_5(\tilde{r})$ can be simplified further by performing the sums to obtain

$$\beta_{5}(\tilde{r}) = (-1)^{(\ell+1)/2} 2^{1+\ell} (1+\ell) (2+\ell) \Gamma(4+\ell) \frac{1}{\tilde{r}^{5+\ell}} \sum_{k=0}^{\ell-2} (-1)^{k} \frac{\Gamma(\ell-k)}{\Gamma(6-k+2\ell)} (\tilde{r}-1)^{k}$$

$$\times \left[(k-2\ell-5) (3+2\ell) (k-4-2\ell) \tilde{r}^{2} {}_{4}F_{3} \left(\frac{\frac{4+\ell}{2}, \frac{5+\ell}{2}, 2+\ell, \frac{5+2\ell}{2}}{\frac{4-k+2\ell}{2}, \frac{5-k+2\ell}{2}}; -\frac{1}{\tilde{r}^{2}} \right) \right]$$

$$-2 (4+\ell) (5+\ell) (5+2\ell) {}_{4}F_{3} \left(\frac{\frac{6+\ell}{2}, \frac{7+\ell}{2}, 3+\ell, \frac{7+2\ell}{2}}{\frac{6-k+2\ell}{2}, \frac{7-k+2\ell}{2}}; -\frac{1}{\tilde{r}^{2}} \right) \right] .$$
 (C.15)

The function $\beta_4(\tilde{r})$ can also be simplified by performing some of the sums in closed form to obtain

$$\beta_{4}(\tilde{r}) = \frac{(-1)^{\ell}}{\Gamma(\ell+1)} (\tilde{r}-1)^{\ell} \sum_{n=0}^{\infty} \alpha_{\ell,n} \frac{(\ell+4+2n)\Gamma(2\ell+4+2n)}{\Gamma(\ell+5+2n)} \left[\ln \left(\frac{\tilde{r}-1}{\tilde{r}} \right) + \frac{1}{\tilde{r}-1} \left(1 - \sum_{k=1}^{\ell+3+2n} \frac{1}{k(k+1)} \frac{1}{\tilde{r}^{k}} \right) \right]$$

$$= \frac{(-1)^{(3\ell+1)/2}}{2} \frac{\Gamma(\ell+3)}{\Gamma(\ell+1)} (\tilde{r}-1)^{\ell-1} \left[1 + (\tilde{r}-1) \ln \left(\frac{\tilde{r}-1}{\tilde{r}} \right) \right]$$

$$+ \frac{(-1)^{\ell+1}}{\Gamma(\ell+1)} (\tilde{r}-1)^{\ell-1} \sum_{n=0}^{\infty} \sum_{k=1}^{\ell+3+2n} \gamma_{\ell,n} \frac{1}{k(k+1)} \frac{1}{\tilde{r}^{k}}, \qquad (C.16)$$

where we have defined

$$\gamma_{\ell,n} := \alpha_{\ell,n} \frac{(\ell+4+2n)\Gamma(2\ell+4+2n)}{\Gamma(\ell+5+2n)} \,. \tag{C.17}$$

The last term in Eq. (C.16) can also be represented as follows:

$$\sum_{n=0}^{\infty} \sum_{k=1}^{\ell+3+2n} \gamma_{\ell,n} \frac{1}{k(k+1)} \frac{1}{\tilde{r}^k} = \frac{(-1)^{(\ell+1)/2}}{2} \Gamma(\ell+3) G\left(\frac{1}{\tilde{r}}, \ell+3\right) \times \\ \times \sum_{j=0}^{\infty} \left(\sum_{n=j+1}^{\infty} \gamma_{\ell,n}\right) \left[\frac{1}{(\ell+4+2j)(\ell+5+2j)} \frac{1}{\tilde{r}^{\ell+4+2j}} + \frac{1}{(\ell+5+2j)(\ell+6+2j)} \frac{1}{\tilde{r}^{\ell+5+2j}}\right], \quad (C.18)$$

where we have defined the new function

$$G(x,N) := \sum_{k=1}^{N} \frac{x^k}{k(k+1)},$$
(C.19)

for some $x \in \Re$ and $N \in \mathbb{N}$. This function is the first N terms of the Taylor series for $1 - \log(1 - x) + x^{-1} \log(1 - x)$ about x = 0. Notice that the sum in this new function is finite, and thus $G(1/\tilde{r}, N)$ is simply a polynomial in $1/\tilde{r}$. Given a particular value of ℓ , the remaining sum over j can be performed explicitly.

Appendix C.2. Radial Series Representation

Instead of using variation of parameters to solve Eq. (23), we will search for a series solution. We thus insert the ansatz

$$\tilde{\vartheta}_{\ell}^{(1/2,0)}(\tilde{r}) = \sigma_1(\tilde{r}) + \sigma_2(\tilde{r}),$$
(C.20)

with

$$\sigma_1(\tilde{r}) := \sum_{n=0}^{\infty} a_{\ell,n} \frac{1}{\tilde{r}^{\ell+1+n}}, \qquad (C.21)$$

$$\sigma_2(\tilde{r}) := \sum_{n=0}^{\infty} b_{\ell,n} \, \frac{1}{\tilde{r}^{\ell+4+2n}} \,,$$
 (C.22)

into Eq. (23) and find recursion relations for the $a_{\ell,n}$ and $b_{\ell,n}$ coefficients.

The recursion relations for the $a_{\ell,n}$ can be solved to obtain

$$a_{\ell,n} = \frac{(\ell+n)!}{\ell! \, n!} \, a_{\ell,0} \,,$$
 (C.23)

which then leads to

$$\sigma_1(\tilde{r}) = \frac{a_{\ell,0}}{(\tilde{r}-1)^{\ell+1}} \ . \tag{C.24}$$

Since this is the leading behavior of the scalar field at large \tilde{r} , we can determine the coefficient $a_{\ell,0}$ by comparing it with the incomplete Beta function representation of the previous subsection:

$$a_{\ell,0} = -\sum_{n=0}^{\infty} \alpha_{\ell,n} B(2n+3,\ell+1) = \frac{(-1)^{\frac{\ell+1}{2}} \sqrt{\pi} \ell!}{2^{\ell}} \left[\frac{(\ell+2)}{\Gamma(\ell+\frac{3}{2})} {}_{2}F_{1}\left(\frac{3}{2},2;\ell+\frac{3}{2};-1\right) - \frac{6}{\Gamma(\ell+\frac{5}{2})} {}_{2}F_{1}\left(\frac{5}{2},3;\ell+\frac{5}{2};-1\right) \right]. \quad (C.25)$$

Resumming the coefficients $b_{\ell,n}$ is more complicated. We can solve the recursion relations to express the $b_{\ell,n}$ coefficient as finite sums that depend on the coefficients $\alpha_{\ell,n}$ in the series expansion of the source:

$$b_{\ell,n} = \frac{\Gamma(\ell+4+n)}{\Gamma(4+n)} \sum_{j=0}^{j_{max}} \frac{\Gamma(3+2j)}{\Gamma(\ell+4+2j)} \alpha_{\ell,j} - \frac{\Gamma(\ell+4+n)}{\Gamma(2\ell+5+n)} \sum_{j=0}^{j_{max}} \frac{\Gamma(2\ell+4+2j)}{\Gamma(\ell+4+2j)} \alpha_{\ell,j} ,$$
(C.26)

where $j_{max} = n/2$ if n is even, and $j_{max} = (n+1)/2$ if n is odd.

When one tries to perform the full infinite sum of the $b_{\ell,n}$ coefficients over n to find $\sigma_2(\tilde{r})$, one finds a familiar problem: the coefficients of Eq. (C.26) are finite sums with an upper limit that depends on n, which must then be summed to infinity. To get around this problem, we can rewrite each finite sum as the difference of two infinite sums:

$$b_{\ell,n} = \frac{\Gamma(\ell+4+n)}{\Gamma(4+n)} c_{\ell,j_{max}} - \frac{\Gamma(\ell+4+n)}{\Gamma(2\ell+5+n)} d_{\ell,j_{max}} , \qquad (C.27)$$

where

$$c_{\ell,k} = (-1)^{\frac{\ell-1}{2}} \frac{\sqrt{\pi}}{2^{\ell+1}} \times \left[\frac{(\ell+1)(4\ell-7)}{2\Gamma(\ell+\frac{3}{2})} + \frac{2(-1)^k(2k+3)\Gamma(k+\frac{5}{2})}{\sqrt{\pi}\Gamma(\ell+\frac{3}{2}+k)} \right]$$

$$+ \frac{(\ell^4 - 2\ell^2 + 9\ell + 10)}{2\Gamma(\ell+\frac{5}{2})} {}_2F_1(-\frac{1}{2}, 1; \ell + \frac{5}{2}; -1) - \frac{(\ell^4 + 5\ell^3 + \ell + 5)}{2\Gamma(\ell+\frac{5}{2})} {}_2F_1(\frac{1}{2}, 1; \ell + \frac{5}{2}; -1) \right]$$

$$+ \frac{2(-1)^k(\ell-1)\Gamma(k+\frac{5}{2})}{\sqrt{\pi}\Gamma(\ell+\frac{5}{2}+k)} {}_2F_1(1, k+\frac{5}{2}; \ell+k+\frac{5}{2}; -1) + \frac{2^{\ell-1}(\ell+2)}{\Gamma(\ell+\frac{3}{2})} {}_2F_1(\ell-\frac{1}{2}, \ell; \ell+\frac{3}{2}; -1) \right] ,$$

$$d_{\ell,k} = (-1)^{\frac{\ell-1}{2}} \times \left[-\frac{1}{2}\Gamma(\ell+3) + \frac{(-1)^k 2^{\ell+2}(k+1)(\ell+k+2)\Gamma(\ell+k+3)}{\Gamma(k+2)} \right] .$$

$$+ \frac{(-1)^k 2^{\ell+1}(\ell+2)\Gamma(\ell+k+3)}{\Gamma(k+2)} {}_2F_1(1, \ell+k+3; k+2; -1) \right] .$$

$$(C.28)$$

With the $b_{\ell,n}$ coefficients expressed in this form, the second sum for the scalar field becomes

$$\sigma_2(\tilde{r}) = \sum_{n=0}^{\infty} \left[\frac{\Gamma(\ell+4+n)}{\Gamma(4+n)} c_{\ell,j_{max}} - \frac{\Gamma(\ell+4+n)}{\Gamma(2\ell+5+n)} d_{\ell,j_{max}} \right] \frac{1}{\tilde{r}^{\ell+4+2n}}.$$
 (C.30)

We have not succeeded in finding closed-form expressions for the sum over n given a generic ℓ value, but the sum can be performed for a given value of ℓ .

Appendix D. Series Solutions for the Trace of the Metric Perturbation

Instead of truncating the Legendre expansion of the scalar field, it is also possible to construct series approximations of the modes $g_{\ell}^{(1,0)}$. We first note that the source term (48) can be expanded in powers of $1/\tilde{r}$. For the $\ell=0$ mode this series takes the form

$$S_0^{(1,0)}(\tilde{r}) = \sum_{n=0}^{\infty} e_{0,n} \frac{1}{\tilde{r}^{4+n}} ,$$
 (D.1)

while for $\ell \geq 2$ it is

$$S_{\ell}^{(1,0)}(\tilde{r}) = \sum_{n=0}^{\infty} e_{\ell,n} \frac{1}{\tilde{r}^{\ell+2+n}}.$$
 (D.2)

In terms of the series coefficients for the source, the $\ell = 0$ mode is

$$g_0^{(1,0)}(\tilde{r}) = \sum_{n=0}^{\infty} e_{0,n} \times \left[\log \left(\frac{\tilde{r}-1}{\tilde{r}} \right) + \sum_{j=1}^{n+3} \frac{1}{j \, \tilde{r}^j} + \frac{1}{n+3} \, \frac{1}{\tilde{r}-1} \left(\frac{1}{\tilde{r}^{n+3}} - 1 \right) \right]. \quad (D.3)$$

Note that the coefficient of the $\log(\tilde{r}-1)$ term is (D.1) evaluated at $\tilde{r}=1$, as in Eq. (60). The modes with $\ell \geq 2$ can be expressed as a series involving incomplete Beta functions:

$$g_{\ell}^{(1,0)}(\tilde{r}) = \sum_{n=0}^{\infty} e_{\ell,n} \times \left[-(\tilde{r}-1)^{\ell} B_{1/\tilde{r}} \left(2\ell + 2 + n, -\ell \right) - \frac{1}{(\tilde{r}-1)^{\ell+1}} B_{1-1/\tilde{r}} \left(\ell + 1, n+1 \right) \right]. \quad (D.4)$$

Since these solutions are obtained directly from Eq. (50) they already satisfy the correct boundary conditions at $\tilde{r} \to \infty$ and $\tilde{r} = 1$.

Given the expansion of the source functions, one can obtain a series solution of the equation of motion Eq. (47) directly. For the $\ell = 0$ mode this solution takes the form

$$g_0^{(1,0)}(\tilde{r}) = \frac{f_{0,0}}{(\tilde{r}-1)} + \sum_{n=0}^{\infty} \frac{1}{\tilde{r}^{4+n}} \sum_{j=0}^{n} \frac{n+1-j}{(n+4)(j+3)} e_{0,j}$$
 (D.5)

while for $\ell \geq 2$ it is

$$g_{\ell}^{(1,0)}(\tilde{r}) = \frac{f_{\ell,0}}{(\tilde{r}-1)^{\ell+1}} + \sum_{n=0}^{\infty} \frac{(\ell+n)!}{\tilde{r}^{\ell+2+n}} \sum_{j=0}^{n} e_{\ell,j} \left(\frac{j!}{(n+1)!(\ell+j+1)!} - \frac{(2\ell+j+1)!}{(\ell+j+1)!(2\ell+n+2)!} \right) . \quad (D.6)$$

In both cases the coefficient $f_{\ell,0}$ of the leading term can be expressed in terms of one or more integrals of the source; for $\ell = 0$ it is

$$f_{0,0} = \int_{-\infty}^{1} d\tilde{r} \, S_0^{(1,0)}(\tilde{r}) \ . \tag{D.7}$$

- Will C M 2014 Living Reviews in Relativity 17 URL http://www.livingreviews.org/ lrr-2014-4
- [2] Yunes N and Siemens X 2013 Living Rev.Rel. 16 [arXiv:1304.3473] URL http://www.livingreviews.org/lrr-2013-9
- [3] Berti E et al. 2015 Class. Quant. Grav. 32 243001 [arXiv:1501.07274]
- [4] Abramovici A et al. 1992 Science 256 325–333
- [5] Giazotto A 1990 Nucl. Instrum. Meth. A289 518-525
- [6] Broderick A E, Johannsen T, Loeb A and Psaltis D (Perimeter Institute for Theoretical Physics) 2014 Astrophys. J. 784 7 [arXiv:1311.5564]
- [7] Weisskopf M C, Brinkman B, Canizares C, Garmire G, Murray S and Van Speybroeck L P 2002 Publ. Astron. Soc. Pac. 114 1–24 [arXiv:astro-ph/0110308]
- [8] Alexander S and Yunes N 2009 Phys.Rept. 480 1–55 [arXiv:0907.2562]
- [9] Delsate T, Hilditch D and Witek H 2015 Phys. Rev. D91 024027 [arXiv:1407.6727]
- [10] Green M B and Schwarz J H 1984 Phys. Lett. B149 117-122
- [11] Green M B, Schwarz J H and Witten E 1988 Superstring Theory. Vol. 2: Loop Amplitudes, Anomalies And Phenomenology (Cambridge: Cambridge University Press) ISBN 9780521357531
- [12] Weinberg S 2008 Phys. Rev. **D77** 123541 [arXiv:0804.4291]
- [13] Taveras V and Yunes N 2008 Phys. Rev. D78 064070 [arXiv:0807.2652]
- [14] Jackiw R and Pi S 2003 *Phys.Rev.* **D68** 104012 [arXiv:gr-qc/0308071]
- [15] Ayzenberg D, Yagi K and Yunes N 2014 Phys. Rev. D89 044023 [arXiv:1310.6392]
- [16] Campbell B A, Duncan M J, Kaloper N and Olive K A 1990 Phys. Lett. B251 34-38
- [17] Yunes N and Pretorius F 2009 *Phys.Rev.* **D79** 084043 [arXiv:0902.4669]
- [18] Konno K, Matsuyama T and Tanda S 2009 Prog. Theor. Phys. 122 561-568 [arXiv:0902.4767]
- [19] Yagi K, Yunes N and Tanaka T 2012 *Phys.Rev.* **D86** 044037 [arXiv:1206.6130]
- [20] Konno K and Takahashi R 2014 Phys. Rev. **D90** 064011 [arXiv:1406.0957]
- [21] Stein L C 2014 Phys. Rev. **D90** 044061 [arXiv:1407.2350]
- [22] Grumiller D and Yunes N 2008 Phys. Rev. **D77** 044015 [arXiv:0711.1868]
- [23] Yunes N and Sopuerta C F 2008 Phys. Rev. D77 064007 [arXiv:0712.1028]
- [24] Sopuerta C F and Yunes N 2009 Phys. Rev. D80 064006 [arXiv:0904.4501]
- [25] Guica M, Hartman T, Song W and Strominger A 2009 Phys. Rev. D80 124008 [arXiv:0809.4266]
- [26] Ghezelbash A M 2009 JHEP 08 045 [arXiv:0901.1670]
- [27] Matsuo Y and Nishioka T 2010 JHEP 12 073 [arXiv:1010.4549]
- [28] Carlip S 2011 JHEP 04 076 [Erratum: JHEP01,008(2012)] [arXiv:1101.5136]
- [29] Compere G 2012 Living Rev. Rel. 15 [arXiv:1203.3561] URL http://www.livingreviews.org/ lrr-2012-11
- [30] Dias O J C, Santos J E and Stein M 2012 JHEP 10 182 [arXiv:1208.3322]
- 31 McNees R and Stein L C Forthcoming
- [32] Kanti P, Mavromatos N, Rizos J, Tamvakis K and Winstanley E 1996 Phys. Rev. D54 5049-5058 [arXiv:hep-th/9511071]
- [33] Alexeev S and Pomazanov M 1997 *Phys. Rev.* **D55** 2110–2118 [arXiv:hep-th/9605106]
- [34] Torii T, Yajima H and Maeda K i 1997 Phys. Rev. D55 739-753 [arXiv:gr-qc/9606034]
- [35] Kleihaus B, Kunz J and Radu E 2011 Phys. Rev. Lett. 106 151104 [arXiv:1101.2868]
- [36] Yunes N and Stein L C 2011 *Phys. Rev.* **D83** 104002 [arXiv:1101.2921]
- [37] Pani P, Macedo C F, Crispino L C and Cardoso V 2011 Phys. Rev. D84 087501 [arXiv:1109.3996]
- [38] Ayzenberg D and Yunes N 2014 *Phys. Rev.* **D90** 044066 [Erratum: Phys Rev.D91,no.6,069905(2015)] [arXiv:1405.2133]
- [39] Misner C W, Thorne K S and Wheeler J A 1973 Gravitation (San Francisco: W. H. Freeman)
- [40] Wald R M 1984 General Relativity (University of Chicago Press)
- [41] Yagi K, Stein L C and Yunes N 2016 Phys. Rev. D93 024010 [arXiv:1510.02152]
- [42] Mercuri S and Taveras V 2009 *Phys.Rev.* **D80** 104007 [arXiv:0903.4407]
- [43] Ali-Haimoud Y and Chen Y 2011 Phys. Rev. D84 124033 [arXiv:1110.5329]
- [44] Yagi K, Stein L C, Yunes N and Tanaka T 2013 Phys. Rev. D87 084058 [Erratum: Phys. Rev. D93,no.8,089909(2016)] [arXiv:1302.1918]
- [45] Kerr R P 1963 Phys. Rev. Lett. 11 237–238

- [46] Stein L C 2014 [arXiv:1407.0744]
- [47] Bardeen J M and Horowitz G T 1999 Phys. Rev. D60 104030 [arXiv:hep-th/9905099]
- [48] GRTensorII this is a package which runs within Maple but distinct from packages distributed with Maple. It is distributed freely on the World-Wide-Web from the address: http://grtensor.org
- [49] Martin-Garcia J M, Portugal R and Manssur L R U 2007 Comput. Phys. Commun. 177 640–648 [arXiv:0704.1756]
- [50] Martin-Garcia J M, Yllanes D and Portugal R 2008 Comput. Phys. Commun. 179 586–590 [arXiv:0802.1274]
- [51] Brizuela D, Martin-Garcia J M and Mena Marugan G A 2009 Gen. Rel. Grav. 41 2415–2431 [arXiv:0807.0824]
- [52] NIST Digital Library of Mathematical Functions http://dlmf.nist.gov/, Release 1.0.10 of 2015-08-07 online companion to [53] URL http://dlmf.nist.gov/
- [53] Olver F W J, Lozier D W, Boisvert R F and Clark C W (eds) 2010 NIST Handbook of Mathematical Functions (New York, NY: Cambridge University Press) print companion to [52]